MASTERARBEIT / MASTER'S THESIS

Titel der Masterarbeit / Title of the Master's Thesis

„MicroCT scanning of Austrian lumbricid earthworm specimens as an attempt for species-level identification of juvenile Lumbricidae (Annelida, Clitellata)“

verfasst von / submitted by

Anna Lanen BEd BA

angestrebter akademischer Grad / in partial fulfilment of the requirements for the degree of

Master of Education (MEd)

Wien, 2023 / Vienna 2023

Studienkennzahl lt. Studienblatt / degree programme code as it appears on the student record sheet:	UA 199 502 507
Studienrichtung lt. Studienblatt / degree programme as it appears on the student record sheet:	Masterstudium Lehramt Sek (AB) Unterrichtsfach Biologie und Umweltkunde Unterrichtsfach Englisch
Betreut von / Supervisor:	ao. Univ.-Prof. Dr. Gerhard Steiner

Table of contents

1. Introduction

With a yearly turnover of up to 25 tons of material per hectare of soil (Westheide & Purschke 2013), earthworms are known for their importance as soil improvers. Earthworms contribute to soil quality through consuming soil along with its bacteria and fungi, plant residues, and feces of decomposers, all pulled into their tunnels from the soil surface. *Lumbricus terrestris*, the common earthworm, burrows tunnels that can be 2-3 meters deep (Peters & Walldorf 1986), which contributes to soil structuring and ventilation. With 200 to 250 individuals per cubic meter in meadows, earthworms are of great importance for litter decomposition, soil structure, and humus formation. Furthermore, with a biomass of up to 100 kg/ha, earthworms are a non-neglectable source of food for various reptiles, birds, amphibians and mammals (Westheide & Purschke 2013). Earthworms are also used in composting processes, which makes them an economically relevant species that is of concern to issues such as sustainable agriculture, food security and climate change (Dominguez et al. 2015).

Earthworms are clitellate annelids, have a segmented tube-shaped, elongated body with a mostly cylindrical cross-section and have eight setae on each segment, arranged paired or distantly paired. The setal arrangement is a diagnostic morphological feature. Their body surface is smooth and moist and can excrete mucus that protects the earthworm from drying out and to glide through its tunnels (Laverack 1963). For burrowing, the first segment of each earthworm is structured with a lobe, referred to as the prostomium. The shape of the prostomium is a diagnostic criterion (Fig. 1 A). Apart from burrowing, the mucus, however, is also of importance for reproduction (Peters & Walldorf 1986). Earthworms are hermaphrodites, like all other Oligochaeta, with a distinct mode of reproduction. Matured specimens usually exhibit a saddle-shaped or circular swelling occurring around the 30th segment, known as clitellum. The position, length and shape of the clitellum varies between species. In some cases, there are swollen humps known as the tubercula pubertatis located on the clitellum. During copulation, both individuals produce a mucus collar at the clitellar region, which surrounds the mating partner. Some species interlock with specialized copulatory setae. Sperm is exchanged through the mucus along external sperm grooves and moved to the partner's receptacles by muscle contraction, resulting in mutual insemination. Self-fertilization does not occur, parthenogenesis is reported, though (Peters & Walldorf 1986; Csuzdi & Zsici 2003). In contrast to polychaetes, reproductive organs of clitellate worms are located only in a few anterior segments (Peters & Walldorf 1986).

1.1 Earthworms in Austria

Lumbricid earthworms have a holarctic distribution and are a dominant soil organism in Europe and in many other temperate areas in the northern hemisphere (Philipps et al. 2019; Rutgers et al. 2016). The family Lumbricidae constitute about 90% of the invertebrate soil biomass in temperate regions (Edwards 2004). According to Westheide & Purschke (2013), there are "about 600 earthworm species worldwide" (Westheide & Purschke 2013: 407).

In Austria, 60 species of lumbricid earthworms are reported (Bauer 2009, Geiser 2018). There are two synoptic identification keys to the earthworms of Austria (Zicsi 1994); Christian & Zicsi 1999) and, more recently, Cszudi & Zicsi (2003) present a comprehensive list of earthworms of Hungary, a neighboring country of Austria. All three keys comprise

descriptions of relevant external and internal morphology for the identification of Austrian earthworms. The following paragraphs will describe the relevant morphology for earthworm identification briefly.

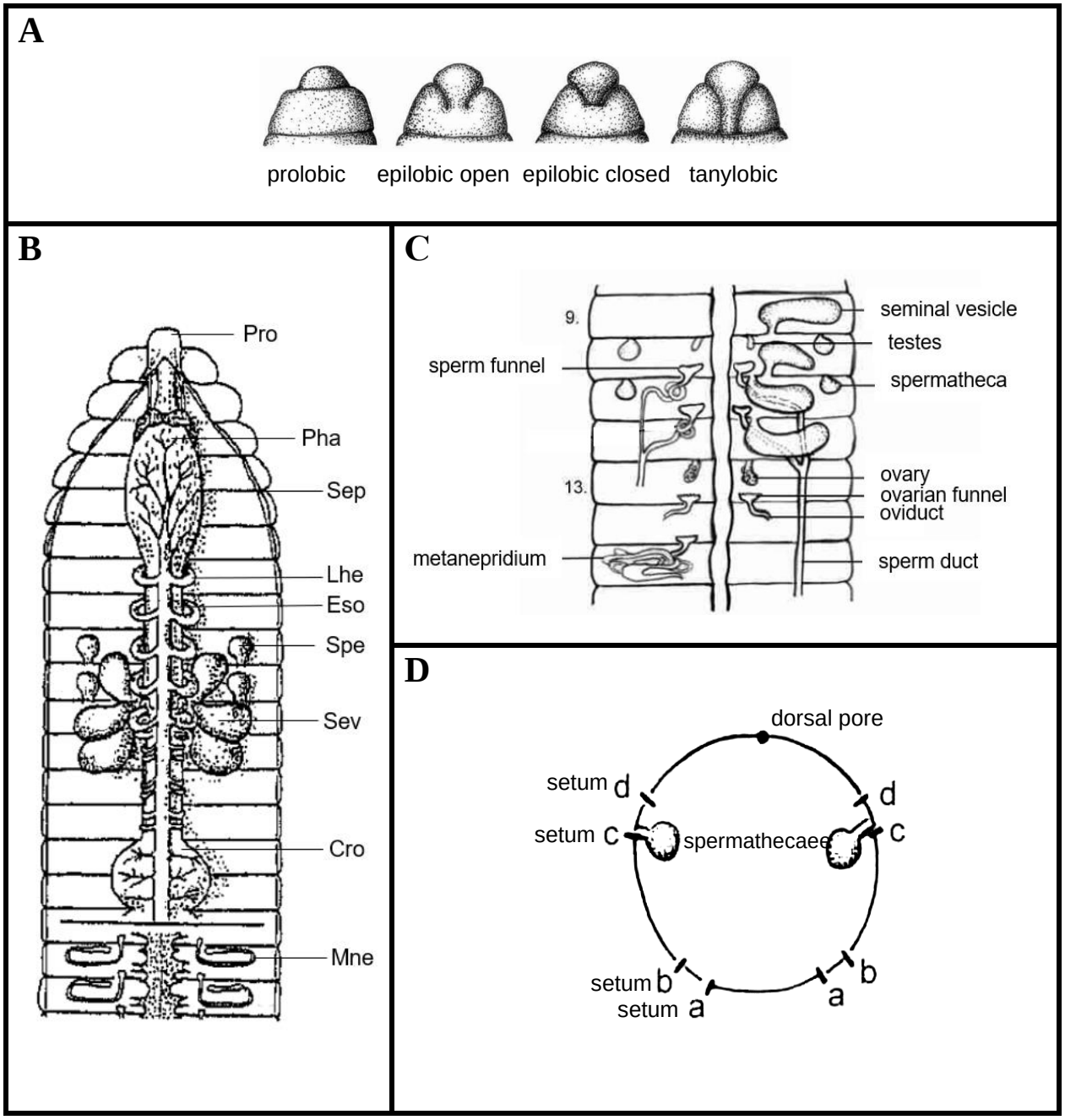

Fig. 1: Earthworm anatomy: (A) Four shapes of the prostomium. (B) Dorsal view on earthworm displaying shape and position of spermathecae and seminal vesicles. (C) Dorsal view of segments 9 to 15 showing testes and ovaries; the seminal vesicles are only displayed on the right side. (D) Schema of a cross-section displaying position of setae, their arrangement (here: paired) and the opening of the spermathecae (here: in setal line c). Images (A), (B), and (D) adapted from Csuzdi & Zicsi (2003), p. 21-33 and image (C) adapted from Christian & Zicsi (1999), p. 123.

In segment 13, most earthworm species have cone-shaped, paired ovaries (Fig 1C). Opposite of each ovary, the oviduct and ovarian funnel are located. Egg cells are transported from the ovaries via the ovarian funnel and oviducts to a ventrally positioned female genital pore, which is located on segment 14 in most species (Csuzdi & Zicsi 2003). The female pore is known to

be inconspicuously for some species (Csuzdi & Zicsi 2003; Peters & Walldorf 1986). In contrast, the male genital pores are prominent in the majority of earthworm species in Austria. The male porus is usually placed ventro-laterally on segment 15. There are exceptions like, *e.g.*, *Eiseniella tetraedra* can have their male porus on segment 13, or on 11, 12, 14 or 15 or "often asymmetrically arranged" (Csuzdi & Zicsi 2003: 154). Another exception is F*itzingeria platyura,* which can have a male porus on segments 26 or 27 (Csuzdi & Zicsi 2003). Most earthworms exhibit swollen tumid lips around the pore. The vasa deferentia, or sperm ducts, are connected to sperm funnels (Fig. 1 C). These lie opposite of the relatively small testes, which are often difficult to see in dissection, as they are surrounded by the seminal vesicles, large structures that can occur in several segments (Figs. 1 B, C). Their location and number is diagnostic for certain genera. For example, all common Hungarian *Octolasion* species show four pairs of seminal vesicles in segments 9, 10, 11 and 12 (Csuzdi & Zicsi 2003). The anterior part of these seminal vesicles is mostly formed with the tissue of the septum between segment 9 and 10, or segment 10 and 11 and the posterior part from the septum between 11 and 12 (Peters & Walldorf 1986). For the storage of external sperm after copulation, earthworms have a varying number of spermathecae (Figs. 1 B, D). These are paired structures and their position and their openings are diagnostic morphological features. For example, *Lumbricus terrestris* exhibits two pairs of spermathecaee in segments 10 and 11 which open between the two most dorsally positioned setae c and d (Fig. 1 D) (Csuzdi & Zicsi 2003). Another characteristic are the dorsal pores that can be found between the segments in the intersegmental furrows. The position of the first dorsal pore (Fig. 1 D) can be diagnostic in some cases. The use of the shape of the typhlosole "has long been debated in earthworm taxonomy" (Csuzdi & Zicsi 2003: 30). It is a dorsally located ridge in the midgut with a lobate cross-section. The shape of this cross-section can be identified for morphological purposes (Csuzdi & Zicsi 2003). Another diagnostic feature of earthworm taxa are the nephridial bladders, a part of the metanephridia (Figs. 1 B, D). For example, *Octolasion* exhibits ocarina-shaped nephridial bladders (Csuzdi & Zicsi 2003). These abovementioned features are commonly described in earthworm literature and identification keys. Together, these features can describe a genus or species. The next section provides an overview the typical features of the three species investigated here: *Octolasion lacteum*, *Fitzingeria platyura*, and *Lumbricus terrestris*.

1.1.1. Genus *Octolasion* ÖRLEY, 1885

Type species – *Lumbricus terrestris* var. *lacteus* ÖRLEY, 1881 (by original or subsequent designation)

Octolasion lacteum (Örley, 1881)

Synonymy:
Lumbricus terrestris var. lacteus ÖRLEY, 1881
Octolasion lacteum ÖRLEY, 1885
Octolasion tyrtaeum: Gates (1973)
Octolasion tyrtaeum gracile: Qui & Bouché (1998)
Octolasion lacteum: Christian & Zicsi (1999); Csuzdi & Zicsi (2003)

For a complete synonymy and nomenclatural discussion see Csuzdi & Zicsi (2003).

To date, *Octolasion tyrtaeum* and *Octolasion lacteum* are accepted synonymized taxa (Rote Liste Zentrum 2023), with both names still in use. This paper uses *Octolasion lacteum*, parallel to the nomenclature from the key that was used (Csuzdi & Zicsi 2003).

Diagnosis: The genus *Octolasion* has ocarina-shaped nephridial bladders. *Octolasion lacteum* has an epilobous prostomium, 1/2 to 2/3 open, and the clitellum is on segments 30 to 35. The setal arrangement behind the clitellum is distantly paired (Csuzdi & Zicsi 2003). Mature individuals have a prominent male genital porus on segment 15 and tubercula pubertatis on segments 31 to 34 (Christian & Zicsi 1999). The internal morphological characteristics that this species shows are four pairs of seminal vesicles in segments 9 to 12 and two pairs of spermathecaee in segments 10 and 11, which open between setae c and d (Csuzdi & Zicsi 2003). In cross-section, the typholosole is anchor-shaped and the longitudinal musculature is of pinnate type. Furthermore, the dissepiments of segments 9/10 and 14/15 are thickened (Csuzdi & Zicsi 2003). *Octolasion lacteum* has calciferous glands in segments 10 and 11 and the first dorsal pore can be located anywhere between intersegmental furrow 8/9 and 11/12 (Christian & Zicsi 1999).

1.1.2. Genus *Fitzingeria* ZICSI, 1978

Type species – *Enterion platyurum* FITZINGER, 1833 (by original designation).

Fitzingeria platyura (FITZINGER, 1833)

Synonymy:
Enterion platyurum FITZINGER, 1833
Helodrilus (Dendrobaena) platyurus: Michaelsen (1900)
Fitzingeria platyura platyura ZICSI, 1978
Dendrobaena platyura platyura: Perel (1979)
Fitzingeria platyura platyura: Zicsi (1991)

For a complete sysnonymy and nomenclatural discussion see Csuzdi & Zicsi (2003).

In comparison to *Octolasion*, the genus *Fitzingeria* has a much less prominent male porus, located near or on the clitellum, a slightly different position of its clitellum, and a differently shaped prostomium: *Fitzingeria* has a clitellum on segments ½ 24 or 25 to 29 or 30, an epilobous ½ closed prostomium, and unpaired setae on segments behind the clitellum (Csuzdi & Zicsi 2003). There in only one known species, *Fitzingeria platyura*, with three subspecies:

(1) *Fitzingeria platyura platyura,* which refers to the original descrition by FITZINGER (1833).
(2) *Fitzingeria platyura depressa* was first described by Rosa (1893) as *Allolobophora platyura depressa*, which has its current name since it was merged with *Fitzingeria platyura quadrivesiculata* by Qui & Bouché (1998).
(3) *Fitzingeria platyura montana*, was first described by Černosvitov (1932) as *Octolasium montanum*, which was then renamed *Dendrobaena platyura* var. *montana* by Pop (1943) and received its current genus assignment by Zicsi (1978).

All information on the nomenclatural history of *Fitzingeria platyura* was derived from Csuzdi & Zicsi 2003). Below, characteristics of the three subspecies of *Fitzingeria platyura* are summarized.

Fitzingeria platyura platyura exhibits an epilobous ½ closed prostomium (Christian & Zicsi 1999). The clitellum is usually positioned on the segments ½ 24 or 25 to 30 with tubercles on segments 25 or 26 to 29. The setal arrangement behind the clitellum is unpaired (Csuzdi & Zicsi 2003). Its male pore is "externally invisible" (Csuzdi & Zicsi 2003: 159), but usually located on segments 26 or 27. It has two pairs of spermathecaee in 9/10 and 10/11 that open in line with setum d. Usually, it has three or four pairs of seminal vesicles in the segments 9 to 12. The nephridial bladders are octahedral in shape and this species has calciferous glands in segments 10 and 11. The typhlosole is unilobate and the longitudinal musculature is pinnate in cross-section. Its first dorsal pore is located somewhere between intersegmental furrows 5/6 - 8/9, usually between 6/7 (Csuzdi & Zicsi 2003). *F. platyura platyura* is known to burrow deeply into the soil and produce humus inside its tunnels and on the earth surface. It is responsible for a litter decomposition of 31 mg dry pass per 1 g body weight and it has a Central-European arboreal distribution (Csuzdi & Zicsi 2003). *F. platyura platyura* is estimated to mature within 12-14 months, and the maximum longevity known is 3 years and 8 months (Csuzdi & Zicsi 2003).

Fitzingeria platyura depressa also has an epilobous ½ closed prostomium, however, it is subject to some variation of the position of its clitellum, which can range from segments 24 or 25 to ½ 30 or 31 (Christian & Zicsi 1999). The setal arrangement behind the clitellum is unpaired and its male genital pore is also usually located on segment 26 but not externally visible. Internally, this subspecies usually it has three pairs of seminal vesicles in segments 9, 11, and 12, and in rare cases four pairs. In contrast to *F. platyura platyura*, this subspecies has three to five pairs of spermathecaee. Its typhlosole, too, is unilobate, the cross-section of the longitudinal musculature is pinnate and it has calciferous glands in segments 10 and 11. Its first dorsal pore is in intersegmental furrows 5/6 or 7/8 (Csuzdi & Zicsi 2003). This subspecies is known to burrow deeply into the soil and produce humus mainly inside its tunnels. It is responsible for a litter decomposition of 25,02 mg dry pass per 1 g body weight. It also has a Central-European distribution (Csuzdi & Zicsi 2003). *F. platyura depressa* has demonstrated a maximum lifespan of 4 years and 5 months and an average of 15-16 months to mature (Csuzdi & Zicsi 2003).

Fitzingeria platyura montana exhibits proepilobous to epilobous prostomium and a clitellum on segments 24 ½ to 30 ½ (Christian & Zicsi 1999). Similar to the other two subspecies, its setal arrangement behind the clitellum is unpaired. Its male genital pore is usually externally invisible but located on segment 25. This subspecies has only two seminal vesicles segments in 11 and 12 and three to five pairs of spermathecael opening in setal line d on segments (6/7, 7/8), 8/9, 9/10, 10/11 (Csuzdi & Zicsi 2003). There are calciferous glands in segments 11 and 12 and the nephridial bladders are octahedral. This subspecies' typhlosole is multilobate and its longitudinal musculature is pinnate. Its first dorsal pore can be located in intersegmental furrow 8/9 or 9/10 (Csuzdi & Zicsi 2003). *F. platyura montana* is also known to burrow deeply and produce humus almost exclusively inside its tunnels. It is responsible for a litter decomposition of 16,7 mg dry mass per 1 g body weight (Csuzdi & Zicsi 2003). Compared to the other two subspecies, *F. platyura montana* has a smaller, "[c]entral-European montane distribution" (Csuzdi & Zicsi 2003: 167). *F. platyura montana* take 12 to 14 months to mature. The maximum longevity known is 6 years and 5 months (Csuzdi & Zicsi 2003).

1.1.3. Genus *Lumbricus* LINNAEUS, 1758

Type species – *L. terrestris* LINNAEUS, 1758 (by subsequent designation (International Commission on Zoological Nomenclature 1922)).

Lumbricus terrestris LINNAEUS, 1758

Synonymy:
Lumbricus terrestris LINNAEUS, 1758
Lumbricus terrestris: Michelsen (1900)
Lumbricus terrestris: Pop (1943)
Lumbricus terrestris: Zicsi (1991)

For a complete sysnonymy and nomenclatural discussion see Csuzdi & Zicsi (2003).

Lumbricus is one of the few genera that has been recognized as monophyletic for several decades (Csuzdi & Zicsi 2003). *Lumbricus terrestris* is the species that is most commonly called "earthworm", although this term often refers to a variety of different, unrelated species.

Diagnosis: *Lumbricus terrestris* has a tanylobous prostomium, its clitellum ranging across the segments 31 or 32 to 37, and its prominent male genital porus on segment 15. The setal arrangement behind the clitellum is closely paired (Csuzdi & Zicsi 2003). There are three pairs of seminal vesicles in segments 9, 11 and 12 and two pairs of spermathecae in segments 10 and 11 that open in setal line cd. The dissepiments of segments 6/7 and 9/10 are thickened and there are calciferous glands in segments 10 to 12. Nephridial bladders are j-shaped, the typhlosole is lamelliform and the longitudinal musculature pinnate (Csuzdi & Zicsi 2003). *Lumbricus terrestris* is of great ecological importance, as this species is known to decompose about 70g dry mass of litter every year and to cast out about 132g of dry pass every year. It is a relatively large species of holarctic distribution (Csuzdi & Zicsi 2003).

1.1.4. Juvenile specimens

Juvenile specimens are earthworms that are not fully matured enough to be sexually reproductive. Externally, juveniles do not exhibit a clitellar swelling or clearly visible genital pores (Christian & Zicsi 1999). There are only the setal arrangement and the shape of their prostomium, and possibly by their body length and pigmentation available for an incomplete identification (Bartlett et al. 2010). In identification keys, therefore, juveniles are often neglected as they do not exhibit these diagnostic morphological features of the sexually mature specimens that are used in these dichotomous keys. For this reason, they are regarded morphologically unidentifiable (Christia & Zicsi 1999; Chang et al. 2009; Römbke et al. 2012; Decaëns 2013; Zott 2014; Domínguez et al. 2015; Philipps et al. 2021) and are excluded from identification attempts.

This is constraining ecological research, as "adult specimens […] often represent only a small percentage of the overall earthworm assemblage" (Bartlett et al. 2010: 69). These two studies highlight this constrain: Meyer & Plankensteiner (1995) collected earthworms in Vorarlberg (Austria) for 5 years and were able to identify 350 adult specimens out of 1598, listing 1248 specimens as "juvenile, not further identifiable specimens" (Meyer and Plankensteiner 1995: 98). In Bauer et al.'s (2008) characterization of the lumbricid fauna east

of Vienna, juvenile earthworms were the dominant group in all four transects with an average 72% of juvenile individuals per m^2 (Bauer et al. 1998: 19) and also not further identified.

With the uprising of genetic identification, a "viable alternative" (Bartlett et al. 2010: 69) to morphological tools was found. It can be applied for any life stage of earthworms, including juvenile specimens (Chang et al. 2009; Decaëns et al. 2013). Using DNA barcoding, Zott (2014), studied 2465 earthworms for their project, out of which 84,5% were juvenile specimen that could now be included in identification. With genetic methods, juvenile specimens can be identified, however, the genetic information alone is not accurate enough to "…solve the current nomenclatural ambiguities in earthworm taxonomy." (Bartlett et al. 2010: 69). To this date, there are hardly any morphological data of juvenile earthworms available. Therefore, a combination of genetic and morphological investigations on juvenile earthworms is a promising approach.

MicroCT scanning is a method for morphological analysis of earthworms that was demonstrated to be effective by Fernàndez et al. (2014), who generated MicroCT images of both museum and freshly fixed adult *Aporrectodea caliginosa* and *Aporrectodea trapezoides* specimens. Their results highlight the benefits of MicroCT scanning: It generates images that can be reconstructed as a three-dimensional volume rendering of the specimen. This volume rendering can be revisited and re-examined anytime, compared to dissection, which needs to be done in one session. Furthermore, the MicroCT data can repeatedly be used to generate views known from histology, such as orthogonal slices, without destroying the specimen. Slices from all regions of interest can be rotated into all possible orientations. As the image data presented by Fernàndez et al. (2014) showed promising resolutions of relevant morphology in adult specimens, the search for the perhaps undeveloped relevant internal morphological characteristics in juvenile specimens is likely to be possible. For this reason, this project will attempt to use MicroCT scanning on juvenile earthworms of selected taxa to test for the presence of internal morphologically features relevant for species identification.

1.2. Research interests

As MicroCT data on Austrian earthworm species are lacking, this study focuses on

(a) testing the power of MicroCT scanning for species identification of adult specimens in selected taxa;
(b) testing the suitability of this method to identify juvenile specimens of these taxa;
(c) verify the MicroCT-based species identification with DNA-barcoding;
(d) contribute MicroCT imaging stacks and a 3D rendering of adult and juvenile specimens to open access databases.

2. Material and Methods

2.1. Specimen collection and preparation

In June 2022, 27 specimens were collected in the public park *Wiener Prater* in Vienna, from the top 15 cm of forest soil (Szederjesi et al. 2018) and transported to the lab in boxes with moist paper towels. After gentle cleaning with water to remove remaining soil particles, specimens were anesthetized in 30% ethanol, and then transferred to 50% ethanol for 15 minutes and finally stored in 70% ethanol. This treatment reduced contractions and shrinkage of the tissues. A few posterior segments were cut off with a scalpel, transferred to 96% ethanol for DNA preservation and stored at -20°C. Subsequently, the worms were fixed in Bouin's fluid

or in formaldehyde overnight. Both fixatives are common and suitable for invertebrates (Metscher 2009). After the fixation, all samples were washed three times with tap water and then submitted to a graded series of ethanol, starting with washes with 30% ethanol, then 2 washes with 50% ethanol and finally with 10 washes with 70% ethanol. All specimens were kept in 20ml glass vials and with the first 7 washes, the 20 ml volume was replaced twice during each wash before leaving the samples in for 30 minutes.

The freshly fixed worms were prepared for MicroCT-scanning. Metscher (2009) recommended contrasting with phosphotungstic acid (PTA) for invertebrates, and it was successfully applied to earthworm specimens by Fernàndez et al. (2014). Following the protocol proposed by Metscher (2009), the working solution was 0.3% PTA in 70% ethanol (Metscher 2009: 4). To allow fast penetration of the contrasting agent into the earthworm tissue, the specimens were cut about 5 segments behind the clitellum, thus keeping the region of interest for species identification intact. Specimens first remained in 0.3% PTA for 4 days and were then transferred back into 70% ethanol. Trial scans showed, however, that parts of the central tissues were not fully stained. Therefore, the samples were stained for another 9 days in 0.3% PTA and then transferred back into 70% ethanol.

2.2 Macroscopic species identification

Using the keys (Höser 2008; Christian & Zicsi 1999) and species descriptions (Csuzdi & Zicsi 2003), the specimens were identified on genus level. Using a binocular, the samples were identified on genus level. The identification was based solely on external morphological characteristics, such as the shape of the prostomium, the location of the clitellum, the setal position behind the clitellum, and the location and prominence of the male genital porus. Due to the conservation with ethanol and partly also due to the fixation with formaldehyde or Bouin's fluid, the tissues showed shrinkage and pigments were altered. Specimen pigmentation, therefore, was not used as a characteristic in the identification process. Body diameter and length was measured, however only the length from prostomium down to segment 32 (measurements in Table 4). The identification of genera was used to decide which specimens were selected for MicroCT scanning and DNA barcoding later. All 6 specimens are deposited in the collection in the Zoological Collection, Department of Evolutionary Biology (University of Vienna, Austria) under the accession numbers UVZC_EV696 (specimen 1), UVZC_EV692 (specimen 2), UVZC_EV693 (specimen 3), UVZC_EV694 (specimen 4), UVZC_EV695 (specimen 5), UVZC_EV691 (specimen 6).

2.3 MicroCT scanning

MicroCT scanners operate with an x-ray source, scintillator-objective lenses and a camera. This method "involves taking many (typically over 1000) x-ray projections (digital radiographs) from different angels around a sample" (Rawson et al. 2020: 1). Samples with low x-ray absorption need to be stained with x-ray absorbing agents. Phosphotungstic acid (PTA), for example, binds to tissue proteins such as fibrin and collagen (Rawson et al. 2020) and scatters the x-ray. The attenuation of the x-ray after passing through the sample is being detected. This data is then reconstructed computationally, producing a 3D greyscale rendering of the volume or 2D segmentation, which is also generated computationally (Rawson et al. 2020). This section will describe the scanning parameters, mounting techniques and 2D and 3D reconstruction methods used to generate the images relevant for this project's research interests.

Fig. 2: SkyScan 1272 micro-CT scanner of the Department of Evolutionary Biology, University of Vienna.

Using the micro-CT-scanner SkyScan1272 (Fig. 2), four selected juvenile and two adult specimens were mounted and scanned, using a tungsten source. Using previously published data (Fernàndez et al. 2014; Lenihan et al. 2014), the scanner was set to the parameters listed below.

2.3.1. Scanning parameters

The x-ray and scanning parameters were a source voltage of 70 kV, source current of 142 µA, an aluminum filter with 0.5 mm, and an image pixel size of 5µm. Exposure was 1010 ms, the rotation step of either 0.100 degrees, always without a 360 degree rotation. Further settings included frame averaging turned on, and random movement turned off. The pixel size in all samples was 5 µm and the reconstruction parameters were smoothing=1, smoothing kernel=2 (Gaussian) and Ring Artefact Correction=12. Depending on the length of the samples, sometimes 2-3 scans needed to be connected. Scanning times varied according to the length of the sample and other settings. Details of the scanning parameters for each sample are included in Table 1.

Table 1: Scanning parameters for the six scans in this project.

	species	stain	pixel size	rotation step [deg]	source voltage and current	filter	approx. scanning duration	sample archiving id.
1	*adult Octolasion lacteum*	PTA	5µm	0.100	70 kV 142 µA	Al 0.5mm	21 hours	UVZC_EV696
2	*adult Fitzingeria platyura platyura*	PTA	5µm	0.100	70 kV 142 µA	Al 0.5mm	18 hours	UVZC_EV692
3	*adult Fitzingeria platyura platyura*	PTA	5µm	0.100	70 kV 142 µA	Al 0.5mm	18 hours	UVZC_EV693
4	*juvenile Fitzingeria platyura platyura*	PTA	5µm	0.100	70 kV 142 µA	Al 0.5mm	21 hours	UVZC_EV694
5	*juvenile Fitzingeria platyura platyura*	PTA	5µm	0.100	70 kV 142 µA	Al 0.5mm	21 hours	UVZC_EV695
6	*juvenile Lumbricus terrestris*	PTA	5µm	0.100	70 kV 142 µA	Al 0.5mm	21 hours	UVZC_EV691

2.3.2. Mounting techniques

Mounting refers to the embedding of tissue in a liquid medium in a container that fits the scanner's dimensions. The specimens were or in 1% low melting temperature agarose gel (with dH_20). The containers varied depending on the thickness of the earthworm. Depending on the earthworms' diameter, fitting plastic pipette tips were used and were heat-sealed at the bottom. These were then filled with the melted agarose and the worms were positioned with their posterior side facing down using tweezers. Once the specimens were fully submerged, the tubes were sealed with parafilm. The tubes were then placed on Lego pieces (Fig. 3) to be placed upright on a matching Lego plate inside the SkyScan 1272 micro-CT-scanner.

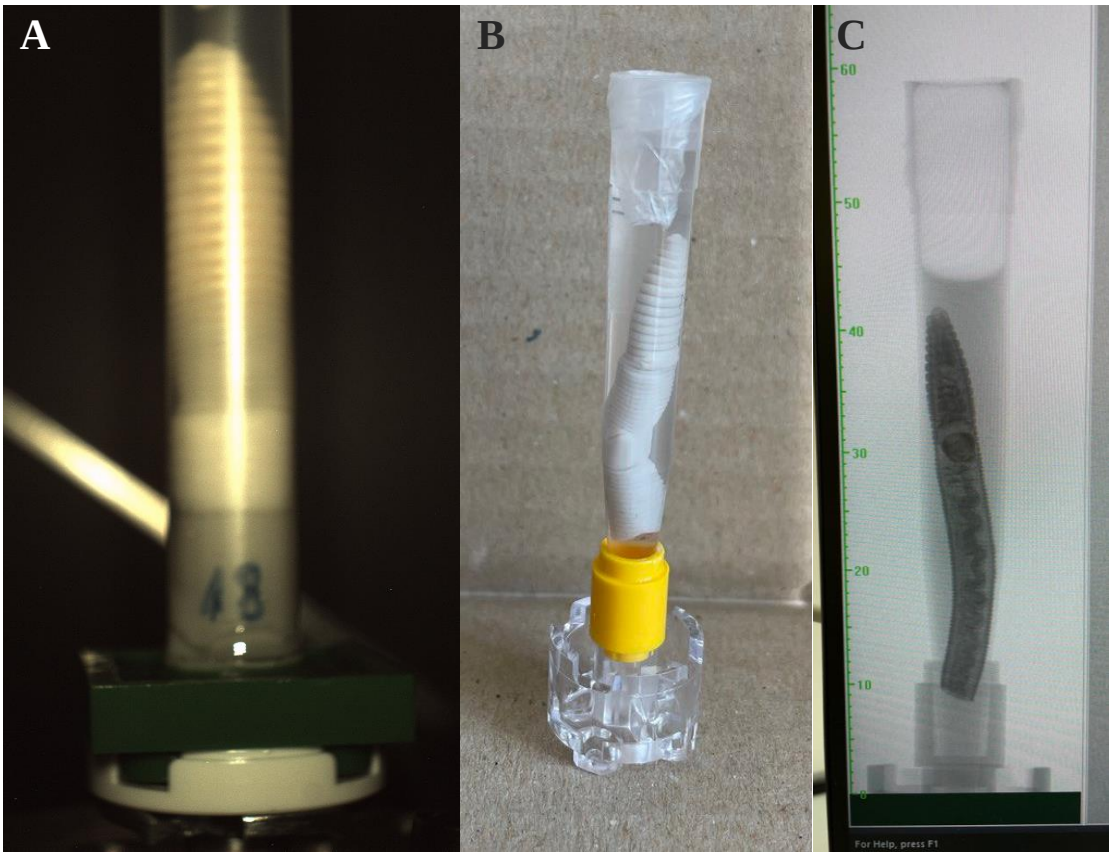

Fig. 3: Mounting designs for earthworms by Brian D. Metscher. (A) A Lego plate functions as the bottom plate within the scanner. (B) The heat-sealed pipette tips are placed in a single Lego piece (see yellow piece in Fig. 3 B above), which were then connected to a pedestal piece (also Lego). (C) Scout scan with x-rays in the SkyScan 1272 scanner, showing that the Lego pieces do not block x-rays.

Using the SkyScan 1272's software, the region of interest was defined, along with all the scanning parameters as listed in Table 1 above. After the scans were done, the image data were reconstructed using the reconstruction program NRecon version 2.0.0.6 (Micro Photonics Inc., Allentown, Pennsylvania, USA). This data then used for 2D and 3D analysis using Amira 2020.2 (Thermo Fisher Scientific, Waltham, Massachusetts, USA).

2.4. 2D and 3D reconstruction

Using Amira's imaging tools, 2D slices and 3D volume renderings were created. These were used for further morphological analysis of species-specific features (see section 3.2.). First, volume renderings were created using the VolRen tool and the GreyScale colour map. The brightness and contrast were adjusted using the histogram bars in the display section reduce Amira's voxel selection to the relevant region. In the VolRen tool properties, specular and top-right light source. To measure the length and diameter of each specimen, snapshots of these volume renderings were measured using Fiji's (Schindelin et al. 2012) measure tool. Then, again using Amira and its Slice tool and its rotate function, three slices oriented to the anatomical planes (transversal, frontal and sagittal) were aligned across the earthworm. Again, the brightness and contrast of each slice were adjusted. In cases of bent worms, the slices were moved across the volume rendering in a way that prioritizes the most relevant areas for morphological identification. Furthermore, scale bars were added. Using Amira's snapshot tool, two-dimensional slices of relevant regions were generated. These images were then later annotated in PowerPoint and overview figures for each scan were created (see section 3.2.).

The relevant morphological structures of one adult and one juvenile *Fitzingeria platyura platyura* specimens were traced for 3D reconstruction with the Amira segmentation tool. The surface renderings of the segmented morphological features were smoothed and embedded in a semi-translucent volume rendering of the specimen (see section 3.2.3.). The imaging stacks are available via Zenodo (European Organization for Nuclear Research; OpenAIRE 2023) under 10.5281/zenodo.8033944 under CC-BY license. 3D reconstructions are available upon request.

2.5. DNA barcoding

Genetic data can be used for species identification and for identifying species boundaries. Sanger sequencing (using a genetic marker and sequencing it) has been used abundantly for analyzing clitellate worms since 1999 (Martinsson & Erséus 2021). The sequence data can be used to generate trees to estimate the phylogenetic relationships and species identities (Briones 2009). For this project, sequences of the commonly used mitochondrial DNA-barcoding marker cytochrome c oxidase subunit 1 (CO1) were generated (Martinsson & Erséus 2021).

Genomic DNA was extracted from the most posterior-most segments using the DNeasy® Blood & Tissue Handbook Protocol: Purification of Total DNA from Animal Tissues (Spin-Column Protocol) (QIAGEN 2020). 1µl of this extracted DNA was then mixed with 15 µl MM Biozym Red HS Taq Master Mix produced by Biozym Scientific GmbH and 13 µl PCR-ready deionized water. The mitochondrial protein coding gene cytochrome c oxidase subunit 1 (CO1) was acquired with polymerase chain reaction (PCR), using each 1 µl of the primers forward and reverse CO1 primers LCO_1490 and HCO_2198, both 20µM (Folmer et al. 1994) and cycled with Biometra TOne. As this standard primer pair did not work for *Octolasion*, new primers were designed and successful applied: OF(5'-ATT CAA CCA ATC ATA AAG ATA TTG G T-3') and OR (5'-AA ACT TCT GGA TGT CCA AAA AAT CA-3'). The cycling specifications are summarized in Table 2.

Table 2: PCR cycling parameters, including temperature [°C], duration [min], and repetition of each step.

temperature [°C]	time [min]	repetition
95	03:00	1
95	00:30	
50	00:30	33
72	00:30	
72	05:00	1
16	hold	

The success of the amplification was determined with gel electrophoresis, using a 1.8% agarose gel with 5µl SYBR safe as a DNA dye. The gel was then loaded with the PCR products and 2µl of the size marker "Quantitas Fast DNA Marker" (Biozym). The electrophoresis ran for 45 minutes at a voltage of 120V.

PCR products were purified by adding 1 µl of Shrimp Alkaline Phosphatase (rSAP) and 1 µl of Exunuclease 1 (Exo I) to remove unused primers and dNTPs. After incubation at 37°C for 5 minutes, enzymes were inactivated at 80°C for 10 minutes, following the A'SAP PCR clean-up manual (ArcticZymes Technologies, 2020). For sequencing, 1 µl of PCR product was added to 3 µl of primer and 11µl of PCR grade water. The samples were sequenced by Microsynth (Vienna, Austria). All 6 CO1 sequences will be made available via GenBank and are available upon request.

Previously published lumbricid CO1 sequences were retrieved from BOLD (Ratnasingham & Herbert 2007) and NCBI databases (NCBI 2023) (accession numbers in Table 5 in section 3.3.) and aligned with the new sequences using the MUSCLE option in Mega X 10.0.5 (Tamura et al. 2021). The best fitting substitution model and the maximum likelihood tree were determined with raxmlGUI 2.0 (Edler et al. 2021). Clade posterior probabilities were inferred with MrBayes 3.2.7 (Ronquist et al. 2012) running 10 million generations under a GTR+G+I model on a single-partition dataset. The sample frequency was set to 100, and the first 6000 sampled trees were discarded as burnin.

3. Results

3.1 Macroscopic genus identification

Out of the 27 collected and freshly fixed specimens, 14 were juvenile and not identifiable with macroscopic methods. The other 13 adult specimens were identified as *Octolasion* (8 specimens), *Fitzingeria* (4 specimens), and *Lumbricus* (1 specimen). Table 3 contains an overview of all visible diagnostic features in each sample. It contains information on the macroscopically visible external features, the relevant internal morphology that was visible in the MicroCT scans, and the genetic information derived from the DNA barcoding.

Table 3: Identification results based on the macroscopically visible morphological characteristics, internal morphology (visible in the MicroCT scans) and the genetic identification. Abbreviations: n.v. (not visible), + (prominent), d (distant), u (unpaired), cp (closely paired).

	taxon of specimen	life stage	macroscopically visible morphological features				visible in CT scans				genetic identification (based on CO1 sequence)
			shape prostomium	position male genital porus [segment]	position clitellum [segment numbers]	setal arrangement (behind clitellum)	shape of typhlosole	spermathecae [number of pairs; segments]	spermathecae opening [setal line]	seminal vesicles [segment numbers]	genus [GenBank accession number(s), % identity]
1	*Octolasion lacteum*	adult	epilobous ½ open	15+	30 - 35	d	anchor-shaped	2x 10, 11	cd	9-12	*Octolasion tyrtaeum* (KM382448, 100%)
2	*Fitzingeria platyura platyura*	adult	epilobous ½ closed	n.v.	25 - 29/30	u	unilobate	2x 10, 11	d	9-12	*Fitzingeria platyura* (KX651141, 98.27%; MZ044882, 98.46%)
3	*Fitzingeria platyura platyura*	adult	epilobous ½ closed	n.v.	24/25 - 29/30	u	unilobate	2x 10, 11	d	9-12	*Fitzingeria platyura* (KX651141, 99.07%; MZ044882, 98.64%)
4	*Fitzingeria platyura platyura*	juvenile	epilobous ½ open	n.v.	n.v.	u	unilobate	2x 10, 11	d	9, 11, 12	*Fitzingeria platyura* (KX651141, 98.12%; MZ044882, 98.45%)
5	*Fitzingeria platyura platyura*	juvenile	epilobous ½ closed	n.v.	25 - 30	u	unilobate	2x 10, 11	d	9-12	*Fitzingeria platyura* (KX651141, 99.07%; MZ044882, 98.64%)
6	*Lumbricus terrestris*	juvenile	tanylobous	n.v.	n.v.	cp	lamelliform	2x 10, 11	cd	9, 11, 12	*Lumbricus terrestris* (HM388349, 100%; OQ743325, 100%)

3.2 MicroCT scanning

The scanning images with the abovementioned scanning parameters were all satisfactory in resoltution for the goals of this project. There was no visible difference between earthworms that were fixed with Formaldehyde or with Bouin's fluid.

3.2.1 Identification of adult specimens

The MicroCT scans show a number of relevant morphological features relevant for species-level identification. Using the most recent key for earthworms of the region (Csuzdi & Zicsi 2003), these were the features that were considered: shape of the prostomium, position of the clitellum, setal arrangement behind the clitellum, position and prominence of the male genital porus, number and position of the seminal vesicles, position of the spermathecae, opening of the spermathecaee, location of the first dorsal pore, location of calciferous glands, shape of the typhlosole and shape of the longitudinal musculature in cross-section. Furthermore, some other characteristics were looked out for that were not visible or even present in all datasets, which are the shape of nephridial bladders and nephridial pore openings. Table 3 gives an overview of the characteristics of each scanned specimen. Specimen lengths from prostomium to segment 33 and diameters are shown in Table 4.

Table 4: Specimen size: Length from prostomium to intersegmental furrow 32/33 and specimen diameter of segment 9. The first three are adult specimens, then three juvenile specimens are listed.

specimen			length up to intersegmental furrow 32/33 [cm]	diameter of segment 9 [cm]
1	**adult**	*Octolasion lacteum*	4.39	0.81
2		*Fitzingeria platyura platyura*	4.64	1.02
3		*Fitzingeria platyura platyura*	4.38	0.95
4	**juvenile**	*Fitzingeria platyura platyura*	4.62	1.01
5		*Fitzingeria platyura platyura*	4.36	0.88
6		*Lumbricus terrestris*	3.78	0.78

All *Fitzingeria platyura platyura* specimens, both in adult and juvenile life stages, are of similar lengths and diameters. The adult *Octolasion lacteum* specimen is similar in length but thinner in diameter than *Fitzingeria platyura platyura* and the juvenile *Lumbricus terrestris* specimen is shorter but thinner in diameter than *Fitzingeria platyura platyura.*

The scan of the adult *Octolasion* specimen (specimen 1) yielded sufficient data for the identification as *O. lacteum*. Fig. 4 shows the epilobous prostomium (Fig. 4 A), the saddle-shaped clitellum on segments 30-35, and band-shaped tubercles across segments 31 to34 (Fig. 4 B), the latter being diagnostic for this species. The male genital porus is located on segment 15 and is surrounded by prominent tumid lips (Fig. 4 B). The setal arrangement in the region behind the clitellum is distantly paired, as the cross-section of segment 37 shows (Fig. 4 C).

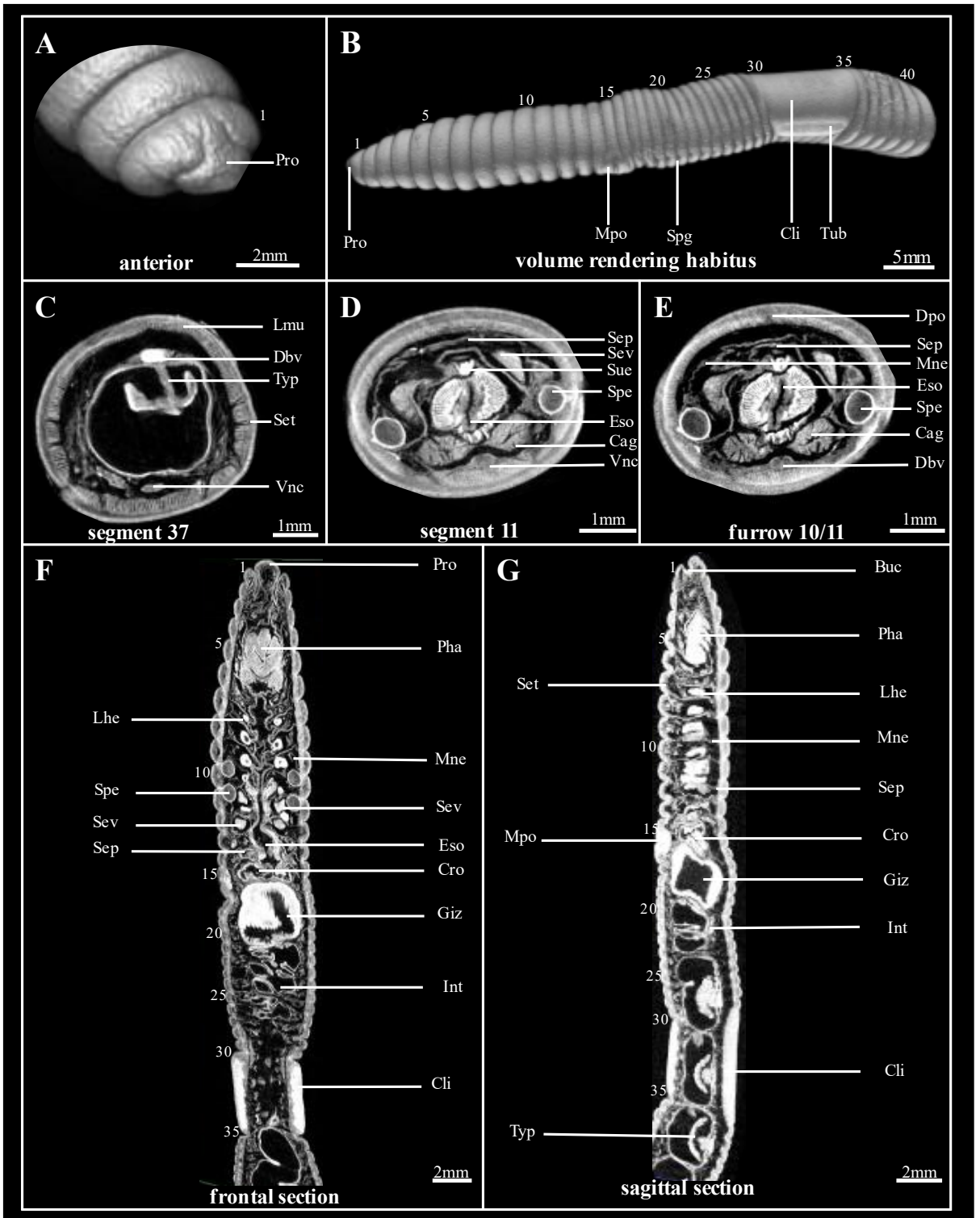

Figure 4: Adult *Octolasion lacteum* (specimen 1). A – volume rendering of the epilobous prostomium; B – volume rendering of the anterior body region showing the position of the clitellum and tubercles; C – 2D slice of segment 37 showing the pinnate longitudinal musculature, distantly paired setae behind the clitellum, and anchor-shaped typhlosole; D – 2D slice of segment 11 showing seminal vesicles and spermathecae; E – 2D slice of intersegmental furrow 10/11 showing the first dorsal pore; F – frontal section displaying the position of spermatheca, seminal vesicles, crop, gizzard and clitellum; G – saggital section displaying position of seminal vesicles, calciferous glands, and clitellum. Abbreviations: Buc (buccal cavity), **Cag** (calciferous glands), **Cli** (clitellum), **Cro** (crop), **Dbv** (dorsal blood vessel), **Dpo** (dorsal pore), **Eso** (esophagus), **Giz** (gizzard), **Int** (intestine), **Lhe** (lateral hearts), **Lmu** (longitudinal musculature), **Mne** (metanephridium), **Pha** (pharynx), **Pro** (prostomium), **Sep** (septum), **Set** (setae), **Sev** (seminal vesicle), **Spe** (spermatheca), **Sue** (supraesophagal vessel), **Tub** (tuberculapubertatis), **Typ** (typhlosole), **Vnc** (ventral nerve cord).

The shape of the typhlosole, as visible in Fig. 4 above, is anchor-shaped and the longitudinal musculature is pinnate (Fig. 4 C). The specimen displays calciferous glands in segments 10 to 12 (Fig. 4 D). The segments 10 and 11 also exhibit a pair of spermathecaee that open between

the setae c and d. Seminal vesicles are present in the segments, 9 to 12. The frontal section (Fig. 4 F) provides an overview of the two pairs of spermathecae in segments 10 and 11. On the ventral side in Fig. 4 G, the male genital porus and its prominent tumid lips are visible on segment 15, as well as the region of the saddle-shaped clitellum on segments 30 to 35. The first dorsal pore is located in the intersegmental furrow 10/11 (Fig. 4 E). The nephridial bladders are visible (Fig. 4 E) but too small for an analysis of their shape. Due to their small size, the nephridiopores were not visible.

The scans of two adult *Fitzingeria* specimens (specimens 2 and 3) allowed for species identification based on a number internal morphological traits. Fig. 5 provides an overview of the characteristics visible specimen 2. The volume rendering of specimen 2 (Fig. 5 A) shows the epilobous prostomium, the circular clitellum extending from segment 25 to 30 and tubercles from segments 26 to 29 (Fig. 5 B) both characteristic for *Fitzingeria platyura*. The cross-section (Fig. 5 C) displays the pinnate nature of the longitudinal musculature layer, the distantly paired setal arrangement of the setae behind the clitellum, and the unilobate shape of the typhlosole. This specimen displays two pairs of spermathecaee in segments 10 and 11, which is typical for the subspecies *Fitzingeria platyura platyura*, as both other subspecies are known to have three or four spermathecael pairs (Fig. 5 F) The openings of the spermathecaee lie in setal line d (Fig. 5 D). Furthermore, this specimen has three pairs of seminal vesicles in segments 9, 11 and 12 (Fig. 5 F and G). The cross-section of segment 11 (Fig. 5 D) shows a pair calciferous glands located ventrally to the esophagus. It further shows seminal vesicles and two spermathecae, which can also be seen in the frontal section (Fig. 5 F). The position of the clitellum and is displayed in (Fig. 5 G), where the brighter line between segments 26 to 29 shows the position of the band-shaped tubercula pubertatis. Another characteristic typical for *Fitzingeria platyura platyura* is the position of the first dorsal pore, which is usually between segments 6/7, which is also visible in this specimen (Fig. 5 E) .It was not possible to locate the male genital porus either specimen. The abovementioned features indicate the subspecies *Fitzingeria platyura platyura.*

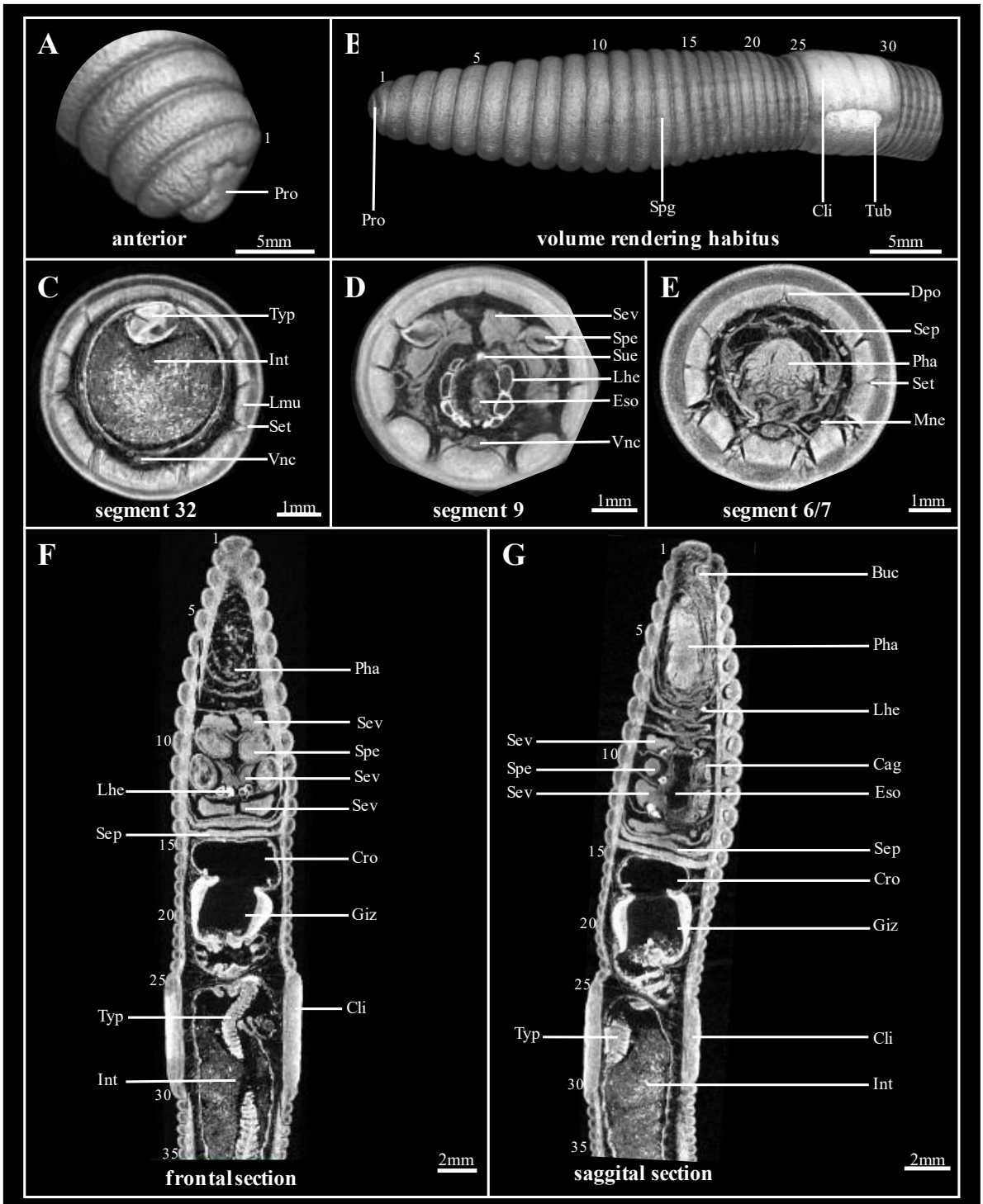

Figure 5: Adult *Fitzingeria platyura platyura* (specimen 2). A – volume rendering of the epilobous prostomium; B – volume rendering of the anterior body region showing the position of the clitellum and tubercles; C – 2D slice of segment 32 showing the pinnate longitudinal musculature, unaired setae behind the clitellum, and unilobate typhlosole; D – 2D slice of segment 9 showing seminal vesicles and spermathecae; E – 2D slice of intersegmentalfurrow 6/7 showing the first dorsal pore; F – frontal section displaying the position of spermathecae, seminal vesicles, crop, gizzard and clitellum; G – saggital section displaying position of seminal vesicles, calciferous glands, and clitellum. Abbreviations: Buc (buccal cavity), **Dpo** (dorsal pore), **Cag** (califerous glands), **Cli** (clitellum), **Cro** (crop), **Eso** (esophagus), **Giz** (gizzard), **Int** (intestine), **Lhe** (lateral hearts), **Lmu** (longitudinal musculature), **Mne** (metanephridium), **Pha** (pharynx), **Pro** (prostomium), **Sep** (septum), **Set** (setae), Sev (seminal vesicle), **Spe** (spermatheca),**Sue** (supraesophagal vessel), **Tub** (tubercula pubertatis), **Typ** (typhlosole), **Vnc** (ventral nerve cord).

3.2.2. Identification of juvenile specimens

Specimens 4 and 5 both are juvenile *Fitzingeria platyura platyura* specimens. Their identification was possible based on a number of visible morphological characteristics in their scans. Both show an epilobous prostomium (Figs. 6 A, B; 7 A, B), and unpaired setal arrangement behind the clitellum (Figs. 6 C, 7 C). Specimen 4 does not show any clitellar swelling (Fig. 6 B) whereas specimen 5 displays onsets of tubercula pubertatis on segments 26 to 29, indicating the future position of the clitellum on this specimen (Fig. 7 B). In cross-section (Figs. 6 C and 7 C), the longitudinal musculature is of pinnate nature and the typhlosole is of unilobate shape. The cross-sections of segment 11 indicate onsets of spermathecaee that open in setal line d in both of these juvenile specimens (Fig. 6 D, 7 D). They are comparatively smaller than in adult specimens, however, their shape and position are indicative of these structures being spermathecaee. Both specimens have calciferous glands ventral to the esophagus in segments 10 and 11 and a first dorsal pore in intersegmental furrow 10/11 (Fig. 6 D and Fig. 7 D). Specimen 5 is quite bent, which is why some sections that need to go through a region of interest do not display the full worm in section. For example, the frontal section of this specimen (Fig. 7 E) is cut off and the sagittal section (Fig. 7 F) does not display the full digestive tract. Several morphologically relevant features are visible nonetheless. Fig. 7 E shows the position of two pairs of spermathecaee in segment 10 and 11. The sagittal section (Fig. 7 F) shows seminal vesicles in four segments 9 to 12. Specimen 4, too, has two pairs of spermathecaee in segments 10 and 11, and onsets of seminal vesicles in segments 9, 11, and 12 (Fig. 6 E, 6 F). There is no trace of a male genital porus in both specimens.

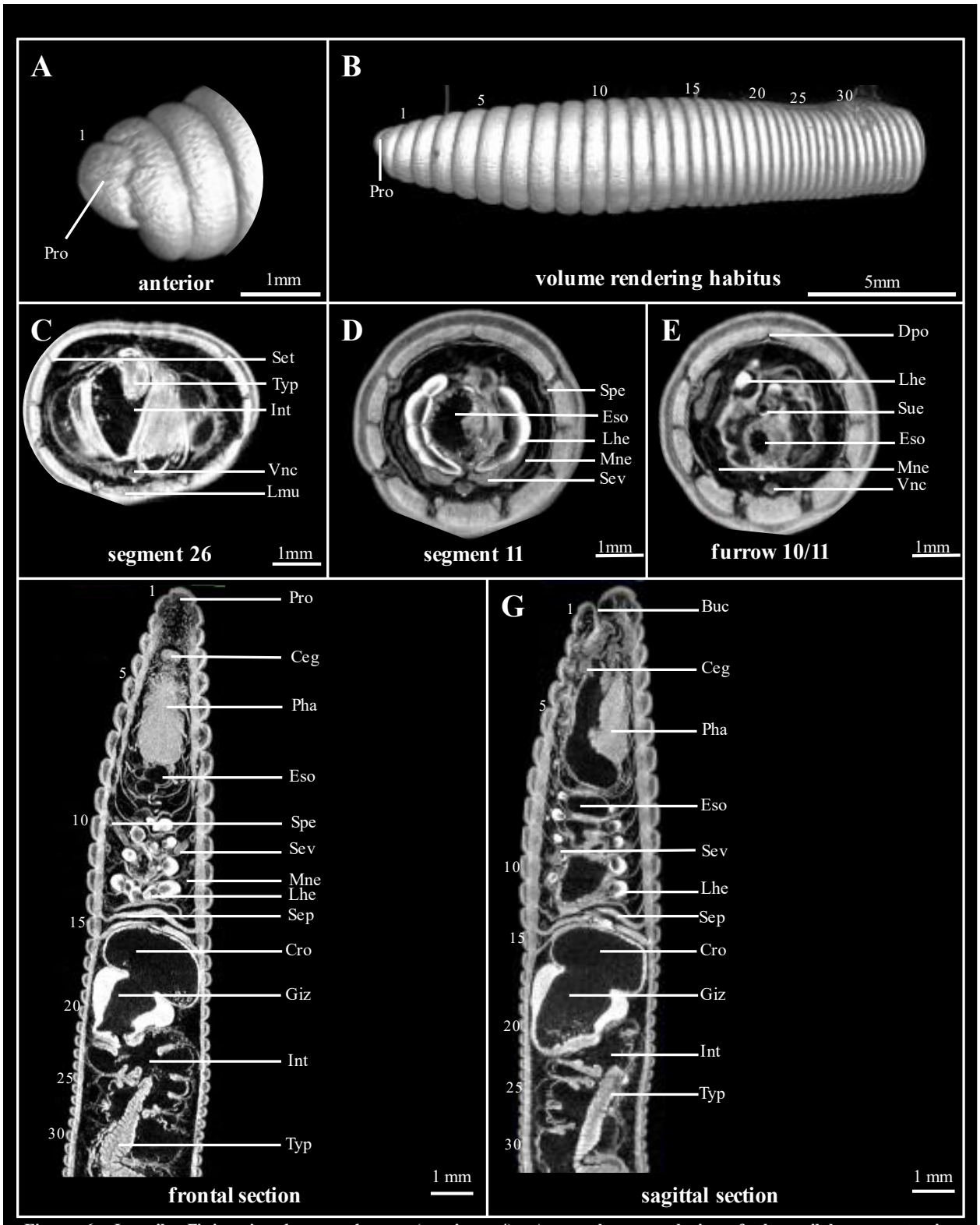

Figure 6: Juvenile *Fitzingeria platyura platyura* (specimen 4): A – volume rendering of the epilobous prostomium; B – volume rendering of the anterior body regions showing no clitellum or tubercles; C – 2D slice of segment 26 showing the pinnate longitudinal musculature, unaired setae behind the clitellum, and unilobate typhlosole; D – 2D slice of segment 11 showing seminal vesicles and spermathecae; E – 2D slice of intersegmental furrow 10/11 showing the first dorsal pore; F – frontal section displaying the position of spermathecae, seminal vesicles, crop, gizzard and clitellum; G – sagittal section displaying position of seminal vesicles
Abbreviations: Buc (buccal cavity), **Ceg** (cerebral ganglion), **Cro** (crop), **Dpo** (dorsal pore), **Eso** (esophagus) **Giz** (gizzard) **Int** (intestine), **Lhe** (lateral hearts), **Lmu** (longitudinal musculature), **Mne** (metanephridia) **Pha** (pharynx), **Sep** (septum), **Pro** (prostomium), **Set** (setae), **Sev** (seminal vesicle), **Spe** (spermatheca) **Typ** (typhlosole), **Vnc** (ventral nerve cord)

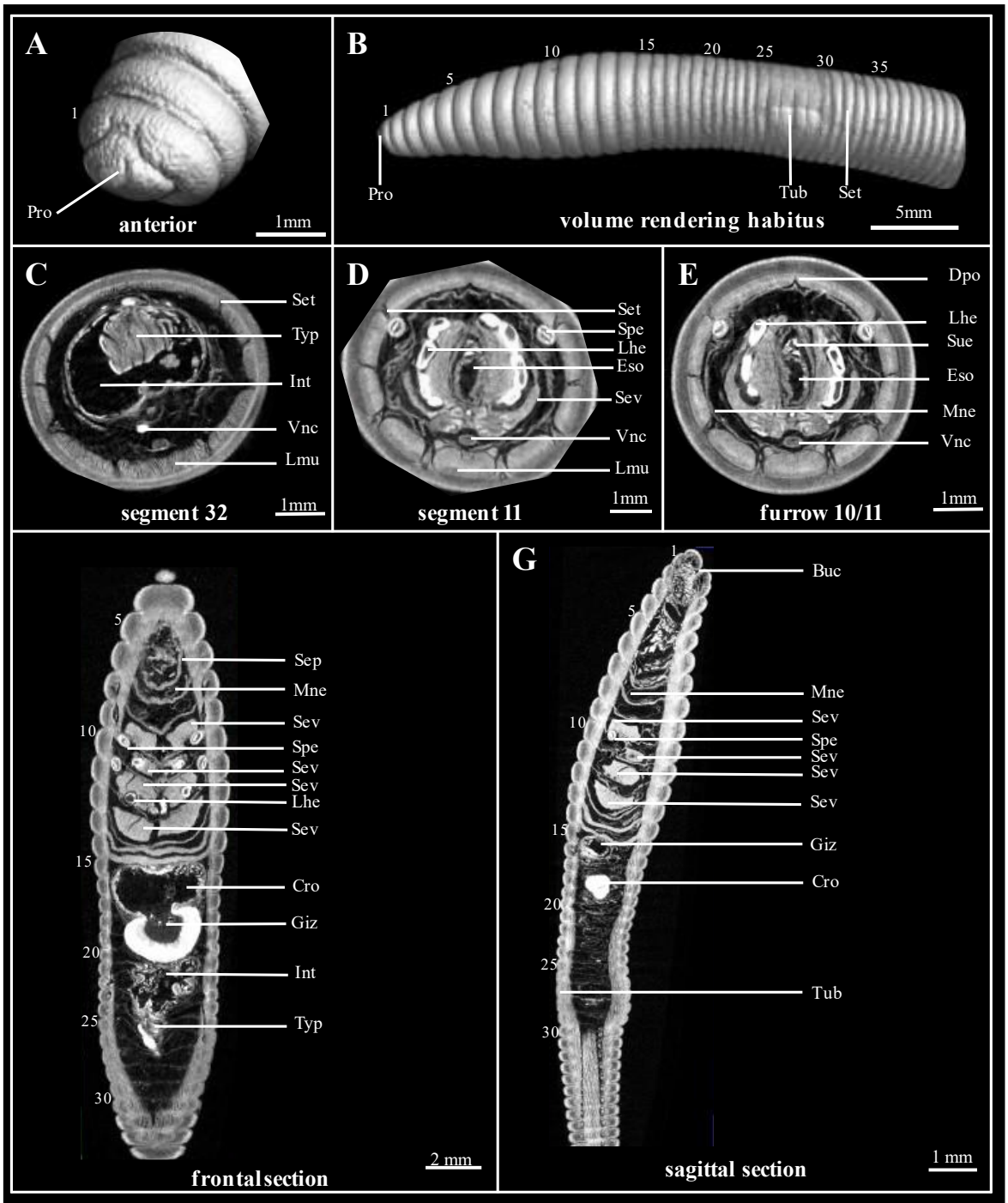

Figure 7: Juvenile *Fitzingeria platyura platyura* (specimen 5). A – volume rendering of the epilobous prostomium; B – volume rendering of the anterior body region showing no clitellum but onsets of tubercles; C – 2D slice of segment 32 showing the pinnate longitudinal musculature, unpaired setae behind the clitellum, and unilobate typhlosole; D – 2D slice of segment 11 showing seminal vesicles and spermathecae; E – 2D slice of intersegmental furrow 10/11 showing the first dorsal pore; F – frontal section displaying the position of spermathecae, seminal vesicles, crop, gizzard; G – saggital section displaying position of seminal vesicles. Abbreviations: Buc (buccal cavity), **Dpo** (dorsal pore), **Cag** (califerous glands), **Cli** (clitellum), **Cro** (crop), **Eso** (esophagus), **Giz** (gizzard), **Int** (intestine), **Lhe** (lateral hearts), **Lmu** (longitudinal musculature), **Mne** (metanephridium), **Pha** (pharynx), **Pro** (prostomium), **Sep** (septum), **Set** (setae), **Sev** (seminal vesicle), **Spe** (spermathecae), **Sue** (supraesophagal vessel), **Tub** (tubercula pubertatis), **Typ** (typhlosole), **Vbv** (ventral blood vessel), **Vnc** (ventral nerve cord).

Considering all morphological features, it is most likely that both specimens belong to *Fitzingeria platyura platyura*. This is supported by DNA-barcoding.

The scan of the juvenile *Lumbricus* specimen (specimen 6), also displayed the presence of several diagnostic features. It has a tanylobous prostomium (Fig. 8 A). Fig. 8 B shows that other than the prostomium, this specimen has no morphologically relevant externally visible characteristics, such as a clitellum or tubercula pubertatis.

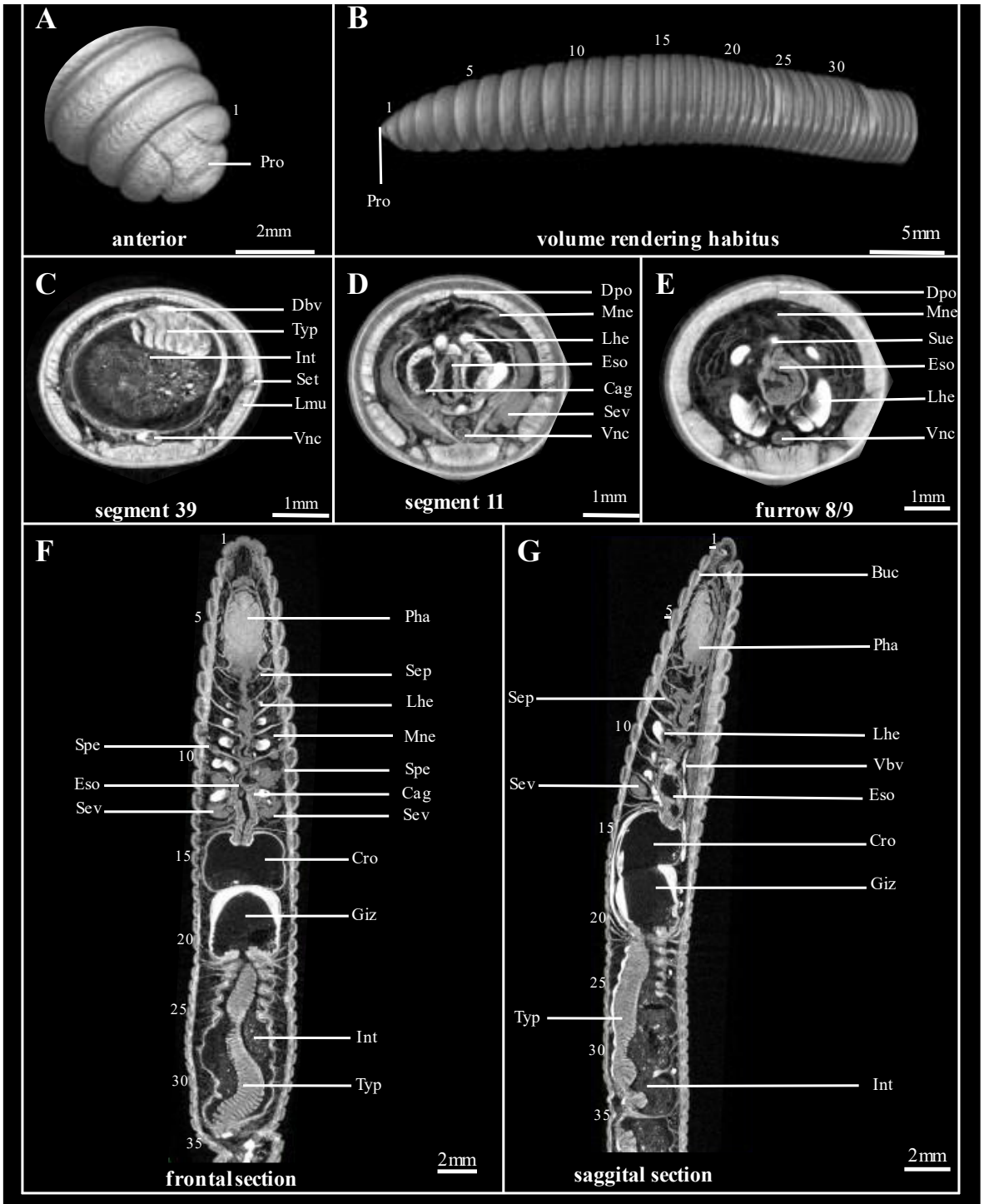

Figure 8: Juvenile *Lumbricus terrestris* (specimen 6). A – volume rendering of the tanylobous prostomium; B – volume rendering of the anterior body region showing no clitellum or tubercles; C – 2D slice of segment 39 showing the pinnate longitudinal musculature, closely paired setae behind the clitellum, and lamelliform typhlosole; D – 2D slice of segment 11 showing seminal vesicles and spermathecae; E – 2D slice of intersegmental furrow 8/9 showing the first dorsal pore; F – frontal section displaying the position of spermatheca, seminal vesicles, crop, gizzard and clitellum; G – saggital section displaying position of seminal vesicles, calciferous glands, and clitellum. Abbreviations: **Buc** (buccal cavity), **Dpo** (dorsal pore), **Cag** (califerous glands), **Cli** (clitellum), **Cro** (crop), **Eso** (esophagus), **Giz** (gizzard), **Int** (intestine), **Lhe** (lateral hearts), **Lmu** (longitudinal musculature), **Mne** (metanephridium), **Pha** (pharynx), **Pro** (prostomium), **Sep** (septum), **Set** (setae), **Sev** (seminal vesicle), **Spe** (spermatheca), **Sue** (supraesophagal vessel), **Tub** (tubercula pubertatis), **Typ** (typhlosole), **Vbv** (ventral blood vessel), **Vnc** (ventral nerve cord).

Based on the literature, the position of the clitellum for *Lumbricus sp.* is between the segments 32 to 37. Therefore, a cross-section (Fig. 8 C) of segment 39 was made to analyze the setal arrangement behind the potential position of the clitellum. Fig. 8 C displays that the setae are closely paired and the cross-section of the longitudinal musculature is pinnate. Furthermore, the typhlosole is lamelliform, and the first dorsal pore is located in intersegmental furrow 8/9, as can be seen in cross-section (Fig. 8 D). In the frontal section (Fig. 8 E), two small pairs of spermathecaee are visible in segments 10 and 11 that open in setal line cd. Furthermore, there are three pairs of seminal vesicles in segments 9, 11 and 12 and calciferous glands in segments 10 to 12, as can be seen in sagittal section (Fig. 8 F). There are no onsets of a clitellum or tubercles visible and there is also no sign of a male genital porus. The position of the first dorsal pore (intersegmental furrow 8/9). Considering all of these morphological features, it is most likely that this specimen is *Lumbricus terrestris.* This is supported by the findings of the DNA barcoding. The results of the DNA barcoding of all scanned specimens are presented in the section 3.3. below.

3.2.3. 3D comparison of juvenile and adult *Fitzingeria platyura platyura* specimens

Reconstructing the diagnostic position of the seminal vesicles, spermathecaee and spermathecael openings three-dimensionally has contributed to the identification of the juvenile specimen. When compared to the adult spermathecaee and seminal vesicle loci (Fig. 9), it becomes evident how much the spermathecaee can increase in size once they are filled with external sperm, reaching a size that extends the segment they originate in (10 and 11). Furthermore, the spermathecael openings could be traced towards the setal line d in both cases, which is the most dorsal setal opening. The seminal vesicles are also smaller in the juvenile worm, yet recognizable in the relevant segments. In comparison to the adult specimen, the lateral hearts are larger in relation to the other organs in the juvenile specimen. Ventral nerve cord and ventral blood vessel serve as orientation markers in the 3D reconstruction.

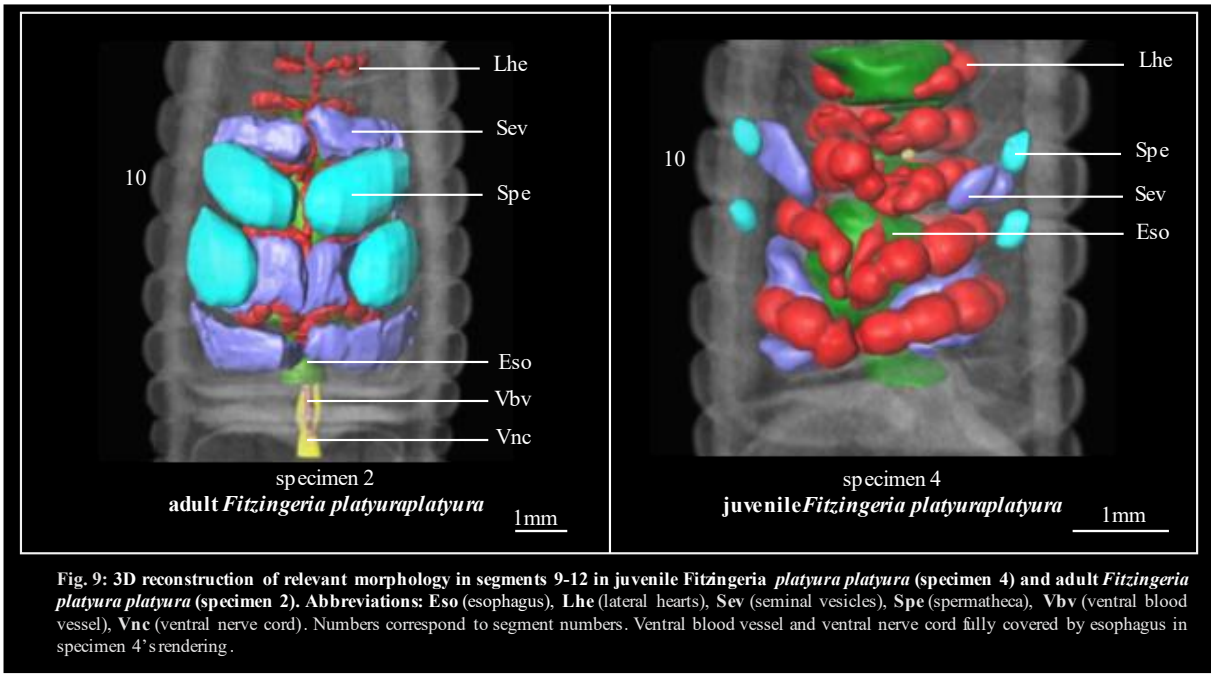

Fig. 9: 3D reconstruction of relevant morphology in segments 9-12 in juvenile Fitzingeria *platyura platyura* (specimen 4) and adult *Fitzingeria platyura platyura* (specimen 2). Abbreviations: Eso (esophagus), **Lhe** (lateral hearts), **Sev** (seminal vesicles), **Spe** (spermatheca), **Vbv** (ventral blood vessel), **Vnc** (ventral nerve cord). Numbers correspond to segment numbers. Ventral blood vessel and ventral nerve cord fully covered by esophagus in specimen 4's rendering.

The 3D renderings of both specimen 2 (adult *Fitzingeria platyura platyura*) and specimen 4 (juvenile *Fitzingeria platyura platyura*) are available upon request.

3.2.4. Anormalities and artifacts

Another interesting observation the difference in the position of the crop and gizzard in the present dataset and the description of the species by Csuzdi & Zicsi (2003). According to them, the crop and gizzard in all genera of this study, *Octolasion*, *Fitzingeria*, and *Lumbricus*, are located in segments 15 to 16 (crop) and 17 to 18 (gizzard). In the present study, however, as Fig. 10 below shows, the musculature of the gizzard extends from segment 17 to about the middle of segment 20. The crop is occasionally locatable in segments 15 to 16, however, this also sometimes reaches into segment 17 on some of the scans.

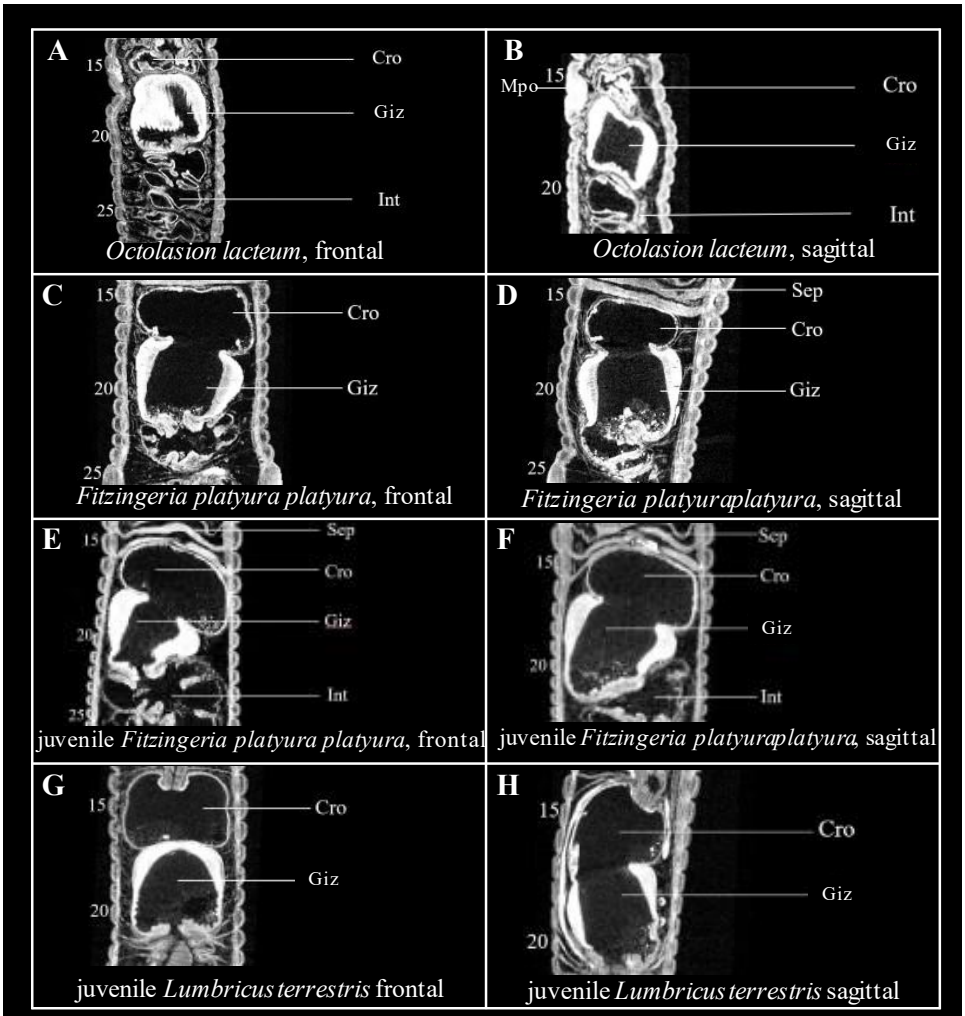

Figure 10: Position of crop and gizzard in the dataset in frontal and sagittal sections. (A) and (B) display relevant segments of *Octolasion lacteum*, (C) and (D) those of an adult *Fitzingeria platyura platyura* specimen, (E) and (F) those of a juvenile *Fitzingeria platyura platyura* specimen, (G) and (H) those of a juvenile *Lumbricus sp.* specimen.
Abbreviations: **Numbers** (refer to segment number), **Cro** (crop), **Giz** (gizzard), **Int** (intestine), **Sep** (septum).

Another insight gained from the process of producing MicroCT scans is which artifacts can occur and how to avoid them. After staining the samples for 4 days initially, the thickest earthworm specimens showed imperfect staining artifacts. These occur in cases where the contrasting agent (in this case: PTA) cannot penetrate the tissue sufficiently. This occurred with two samples of adult *Fitzingeria platyura platyura* specimens; Fig. 11 A-C below showing one of them. Both incompletely stained specimens were restained for another 9 days in PTA.

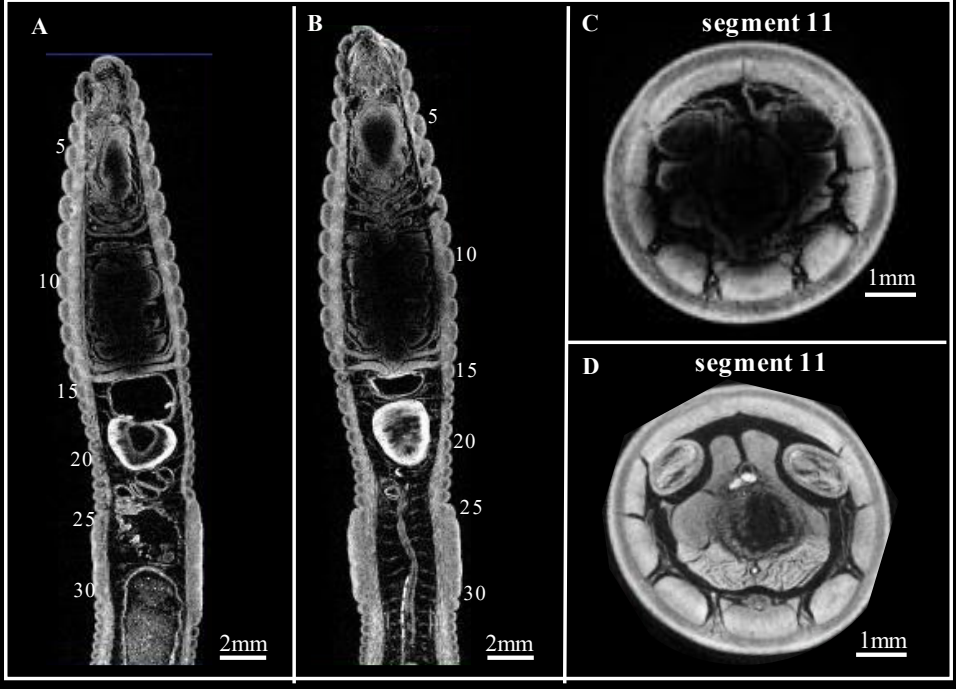

Figure 11: Incomplete staining artefacts(A-C) in scan of specimen 2 after staining in PTA (phosphotungstic acid) for 4 days: (A) Frontal view, (B) saggital view and (C) transversal section at segment 11, revealing a dark cloud across the thickest section f the worm, indicating incomplete staining. (D) Transversal section of segment 11 after a total of 13 days in PTA, revealing complete staining of the tissue.

3.3 Verification with DNA-barcoding

For this step, the posterior ends of each specimen were used for CO1-sequencing and database comparison. Table 5 below lists the results of the DNA barcoding procedure and the genetic overlap with previously published database entries (see Fig. 12).

Table 5: First hits of searches for CO1 sequence nucleotide blast (NCBI 2023) and species identification request (BOLD; Ratnasingham & Herbert 2007). Genetic identity given in brackets. Reference dataset referred to with GenBank accession number. List sorted by scanning order of the present project.

scan number	**taxon**	**COI blast first hit (% identity)** (NCBI 2023)	**GenBank accession number**	**CO1 BOLD first hit (% identity)** (Ratnasingham & Herbert 2007)	**GenBank accession number**
1	*Octolasion lacteum*[1]	*Octolasion tyrtaeum* (99.84%)	KM382448	*Octolasion tyrtaeum* (100%)	KM382448
2	*Fitzingeria platyura platyura*	*Fitzingeria platyura (98.*27%)	KX651141	*Fitzingeria platyura* (98.46%)	MZ044882
3	*Fitzingeria platyura platyura*	*Fitzingeria platyura* (99.07%)	KX651141	*Fitzingeria platyura* (98.64%)	MZ044882
4	*Fitzingeria platyura platyura,* juvenile	*Fitzingeria platyura* (98.12%)	KX651141	*Fitzingeria platyura* (98.45%)	MZ044882
6	*Fitzingeria platyura platyura,* juvenile	*Fitzingeria platyura* (99.07%)	KX651141	*Fitzingeria platyura* (98.64%)	MZ044882
5	*Lumbricus terrestris,* juvenile	*Lumbricus terrestris* (100%)	HM388349	*Lumbricus terrestris* (100%)	OQ743325

These results verify the MicroCT-scanning-based species identification results from section 3.2 above.

[1] *Octolasion tyrtaeum* (SAVIGNY 1826) and *Octolasion lacteum* are synonymized taxa (Rote Liste Zentrum 2023). This paper uses the most recent name (*Octolasion lacteum*, ÖRLEY 1881), as this is also the name used in Csuzdi & Zicsi (2003). Therefore, all of the database species identification results correspond with this projects' species identification.


0.2

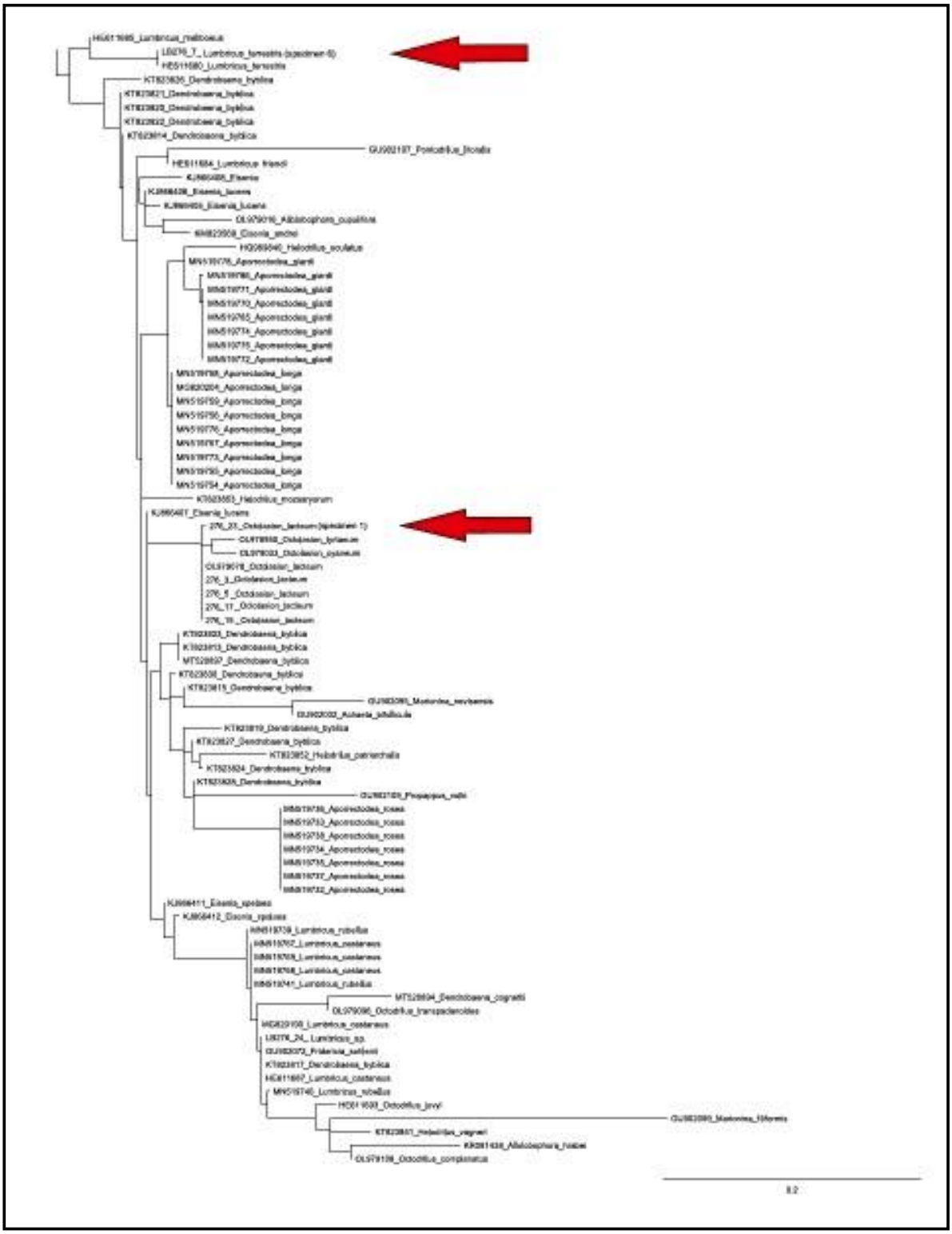

Figure 12: Maximum likelihood tree from CO1 sequences (-Ln = 4591.212). The positions of the specimens examined and the closest relatives are indicated by arrows. GenBank accession numbers precede the taxon names.

The maximum-likelihood tree of the CO1 sequences is optimized with the best-fit model TIM3+I+G4 (Fig. 12; -Ln = 4591.212). It shows *Octolasion lacteum* (specimen 1) in a clade of highly similar sequences of the same species and of *O. tyrtaeum* and *O. cyaneum*. The specimens of *Fitzingeria platyura platyura* (specimens 2 to 5) are monophyletic and closely related to the published sequences of *F. platyura* (as *Dendrobaena*) and unnamed *Dendrobaena* species. The *Lumbricus terrestris* sequence is identical to the only other published one. The three relevant clades have 1.0 posterior probability.

4. Discussion

Overall, species identification with MicroCT scanning of earthworms was possible and all four research interests could be pursued. The most relevant features were visible, however, there are some limitations to this process. Both aspects will be discussed below.

The majority of relevant morphological features was made visible with this projects' methodology. As Table 3 listed above, the shape of the typhlosole, the position and opening of the spermathecae and the position of the seminal vesicles were clearly visible. The three adult specimens could be identified using MicroCT scanning and verified with DNA barcoding. Research interest (a) was therefore successful. This procedure was replicable for the identification of juvenile earthworms, and it was possible to identify three juvenile specimens using MicroCT scanning. Therefore, research interest (b) could also be carried out. The results of the DNA barcoding procedure for the juvenile specimens further support the successful species identification of juvenile earthworms, which makes research interest (c) also a success. The specimens themselves, their imaging data and their CO1 sequences were made available in databases, fulfilling research interest (d). Within the process of Micro-CT-based identification, however, there were some limitations to the method and some artifacts that occurred during the process of scanning.

Some systematically important features were not visible, such as the shape of the nephridial bladders or details of the female reproductive organs. The SkyScan1272 system has a practical resolution limit of 2 to 3µm voxels and any structures around and below this size cannot be resolved in detail, if at all. This applies to structures such as the male genital pores of *Fitzingeria platyura platyura*, which are known to be inconspicuously small (Csuzdi & Zicsi 2003). Furthermore, structures that have too little contrast can also be poorly or not at all visible. Being small in nature too, and perhaps not contrasted sufficiently, the female porus as well as the nephridial bladders might be poorly visible for this reason.

For the abnormalities in the size of crop and gizzard, a possible reason could be that Csuzdi & Zicsi (2003) derived their data mainly from dissections, in which crop and gizzard were only seen in those segments in which they were attached to. In contrast, the MicroCT scans enable to see the position of the structures in intact three-dimensional space, which is why they also show the tips and ends of the gizzard, resulting in the organ looking larger than it was described by Csuzdi & Zicsi (2003). Another reason could be that the gizzard and crop are by themselves actually smaller, and that the connecting musculature is not regarded as part of the organ by Csuzdi & Zicsi (2003). If that is the case, however, the key might need to be extended and some MicroCT scanning data might need to be added for further clarity.

In conclusion, this project succeeded in species-level identification of three juvenile earthworms of the three species. This number is too low to allow for any generalizations. Most of the relevant morphological features were visible, and identification was possible, however, some other relevant features were not visible (e.g. nephridial bladders, female genital porus, testes, and in case of *Fitzingeria platyura platyura*: male genital porus). This might be due to the MicroCT scanning resolution limit, but could also be due to the lack of training of the author. Therefore, further research attempts to see these structures would be necessary. Furthermore, the species in this project, *Fitzingeria platyura platyura* and *Lumbricus terrestris*, are relatively large earthworm species. It would be interesting to see if juvenile specimens of smaller species (e.g. *Eiseniella*) could also be identified using MicroCT scanning. Furthermore, it would be interesting to attempt multi-specimen scans (several juvenile earthworms mounted at once) to try identification with more specimens, potentially even faster. The images that were generated in this project could serve as comparative data. Furthermore, the images and the 3D reconstruction could be used for educational purposes, such as teaching imaging techniques or earthworm anatomy. Given the high abundance of juvenile specimens in earthworm collections (as was outlined in section 1.1.4 above), there might be some implications on ecological or faunistic questions, as this project's method demonstrated that identification of juvenile specimes might be possible. Finally, as the specimens presented in this paper are still intact, there is still the option of dissecting in case of other questions arising that might dissection. In sum, there are some clear benefits to using MicroCT scanning as a method for earthworm identification, especially the possibility of juvenile specimen identification. This potential might be analyzed and tested in further research. Since MicroCT scanning has been successfully applied to museum specimens (Fernàndez et al. 2014), juvenile museum earthworm specimens could potentially also be identified in future research. Despite having only applied MicroCT scanning to three juvenile earthworms, this project has shown that it is not impossible to identify juvenile earthworms.

5. References

Bährmann, R. & Müller, H. (Eds.). (2008). *Bestimmung wirbelloser Tiere: Bildtafeln für zoologische Bestimmungsübungen und Exkursionen* (in German; translated title: Identification of invertebrates: Images for zoological identification practie and excursions). (5th ed.), Heidelberg: Spektrum Akademischer Verlag.

Bauer, R.; Küpper, K.; Müller, E. (1998). „Characterization of the lumbricid fauna in alluvial soils in the Danube River floodplain area east of Vienna". *Linzer Biologische Beiträge* (0030_1), 11–20.

Bauer, R. (2009). "Annelida (Ringelwürmer). Enchytraeidae (Enchyträen)". In: Rabitsch W. & Essl F. (Hg.), *Endemiten. Kostbarkeiten in Österreichs Pflanzen- und Tierwelt.* Klagenfurt u. Wien: Naturwiss. V. f. Kärnten u. Umweltbundesamt GmbH, 308–311.

Bartlett, M.; Briones, M; Creamer, R.; Neilson, R.; Schmidt, O.; Spurgeon, D. (2010). "A critical review of current methods in earthworm ecology: From individuals to populations". *European Journal of Soil Biology* 46 (2), 67–73.

Bouché, M. (1972). "Lombriciens de France: écologie et systématique" (in French, translated title: Lumbricid earthworms of France: Ecology and Systematics). *Institut National de la Recherche Agronomique, publication* (72–2), 672 pp.

Briones, I. M. J.; Moran, P.; Posada, D. (2009). "Are the sexual, somatic and genetic characters enough to solve nomenclatural problems in lumbricid taxonomy?" *Soil Biology and Biochemistry*, 41(11), 2257–2271.

Černosvitov, L. (1935). Monografie československých deštovek (in Czech; translated title: Monograph of Czechoslovak earthworms). *Archiv pro přírodovědecký výzkum Čech*, 19: 1–86.

Černosvitov, L. (1937). "On a collection of Indian earthworms of the family Lumbricidae". *Records of the Indian Museum* (39), 105–111.

Chang, C.; Rougerie, R.; Chen, J.-H. (2009). "Identifying earthworms through DNA barcodes: Pitfalls and promise". *Pedobiologia*, 52(3), 171–180.

Christian, E., & Zicsi, A. (1999). Ein synoptischer Bestimmunggschlüssel der Regenwümer Österreichs (Oligochaeta: Lumbricidae) (in German; translated title: A synpotic identification key of Austrian earthworms (Oligochaeta: Lumbricidae)). *Bodenkultur* 50, 121-131.

Csuzdi, C., & Zicsi, A. (2003). *Earthworms of Hungary (Annelida: Oligochaeta, Lumbricidae).* Budapest: Hungarian Natural Museum and Systematic Zoology Research Group of the Hungarian Academy of Sciences.

Decaëns, T.; Porco, D.; Rougerie, R.; Brown, G. G; James, S. W. (2013). "Potential of DNA barcoding for earthworm research in taxonomy and ecology". *Applied Soil Ecology* 65, 35–42.

Domínguez, J., Aira, M., Breinholt, J. W., Stojanovic, M., James, S. W., & Pérez-Losada, M. (2015). "Underground evolution: New roots for the old tree of lumbricid earthworms". *Molecular Phylogenetics and Evolution* 83, 7–19.

Edwards, C. A. (Ed.). (2004). *Earthworm Ecology* (2nd ed.). Baton Rouge: Taylor & Francis Group.

Edler, D.; Klein, J.; Antonelli, A.; Silvestro, D. (2021). "raxmlGUI 2.0: A graphical interface and toolkit for phylogenetic analyses using RAxML". *Methods in Ecology and Evolution* 12, 373– 377.

European Organization for Nuclear Research, & OpenAIRE. (2013). Zenodo. Available via https://doi.org/10.25495/7gxk-rd71 (latest access June 15th 2023).

Fernández, R., Kvist, S., Lenihan, J., Giribet, G., & Ziegler, A. (2014). „Sine systemate chaos? A versatile tool for earthworm taxonomy: Non-destructive imaging of freshly fixed and museum specimens using micro-computed tomography". *PloS One* 9 (5).

Fitzinger, L. (1833). "Beobachtungen über die Lumbrici". *Isis* (4), 549-553.

Folmer, O.; Black, M.; Hoeh, W.; Lutz, R.; Vrijenhoek, R. (1994). "DNA primers for amplification of mitochondrial cytochrome c oxidase subunit I from diverse metazoan invertebrates". *Molecular Marine Biology Biotechnology* 10/3 (5): 294-299.

Geiser, E. (2018). "How Many Animal Species are there in Austria? Update after 20 Years". *Verhandlungen Der Zoologisch-Botanischen Gesellschaft in Wien* (155_2), 1–18.

Höser, N. (2008). „Lumbricidae. Regenwürmer: nur geschlechtsreife Tiere". In R. Bährmann & H. J. Müller (Eds.), *Bestimmung wirbelloser Tiere: Bildtafeln für zoologische Bestimmungsübungen und Exkursionen* (5th ed.), Heidelberg: Spektrum Akademischer Verlag, 6–7.

International Commission on Zoological Nomenclature. (1922). "Opinion 75. Twenty-Seven Generic Names of Protozoa, Vermes, Pisces, Reptilia and Mammalia Included in the Official List of Zoological Names". *Smithsonian Miscellaneous Collections* 73 (1), 35–37.

Kumar, S.; Stecher, G.; Li, M.; Knyaz, C.; Tamura, K. (2018). „MEGA X: Molecular Evolutionary Genetics Analysis across computing platforms". *Molecular Biology and Evolution* 35, 1547-1549.

Lenihan, J.; Kvist, S.; Fernández, R.; Giribet, G.; Ziegler, A. (2014). „A dataset comprising four micro-computed tomography scans of freshly fixed and museum earthworm specimens". *GigaScience* 3 (1), 1-4.

Laverack, M. (1963). *The Physiology of Earthworms: International Series of Monographs on Pure and Applied Biology: Zoology*. Burlington:. Elsevier Science.

Martinsson, S. & Erséus, C. (2021). "Cryptic Clitellata: Molecular Species Delimitation of Clitellate Worms (Annelida): An Overview". *Diversity*, *13*(2), 36.

Metscher, B. D. (2009). "MicroCT for comparative morphology: Simple staining methods allow high-contrast 3D imaging of diverse non-mineralized animal tissues". *BMC Physiology* 9, 11.

Meyer, E., & Plankensteiner, U. (1995). „Regenwürmer (Lumbricidae) in Waldböden Vorarlbergs (Österreich)" (in German; translated title: Earthworms (Lumbricidae) in forest soils of Vorarlberg (Austria)). *Berichte Des Naturwissenschaftlichen-Medizinischen Verein Innsbruck* (82), 95–103.

Michaelsen, W. (1900). *Das Tierreich. Eine Zusammenstellung und Kennzeichnung der rezenten Tierformen. Oligochaeta* (in German; translated title: The animal kingdom. An overview and nomenclature of recent animals. Oligochaetes.) Berlin, Germany: Friedländer & Sohn, 488-575.

Micro Photonics Inc. (2023). *NRecon version 2.0.0.6.* Allentown, Pennsylvania, USA.

NCBI (National Center for Biotechnology Information). Bethesda (MD): National Library of Medicine (US), *National Center for Biotechnology Information (NCBI)*. 2023 Available from https://blast.ncbi.nlm.nih.gov/Blast.cgi (last visited May 21st 2023).

Örley, L. (1881): "Amagyarországi Oligochaeták faunája. I. Terricolae" (in Hungarian; translated title: Hungarian oligochaete fauna). *Mathematikai és Természettudományi Közlemények* 16: 562–611.

Peters, W., & Walldorf, V. (1986). *Der Regenwurm - Lumbricus terrestris L: Eine Praktikumsanleitung*. Heidelberg: Quelle u. Meyer.

Perel, T.S. (1976). "Dendrobaena (part.)" *Zoologicheskii Zhurnal* (55): 835.

Phillips, H. R. P., Guerra, C. A., Bartz, M. L. C., Briones, M. J. I., Brown, G., Crowther, T. W., Ferlian, O., Gongalsky, K. B., van den Hoogen, J., Krebs, J., Orgiazzi, A., Routh, D., Schwarz, B., Bach, E. M., Bennett, J., Brose, U., Decaëns, T., König-Ries, B., Loreau, M., . . . Eisenhauer, N. (2019). "Global distribution of earthworm diversity". *Science (American Association for the Advancement of Science)*, 366 (6464), 480–485.

Pop, V. (1943). "Hazai és külföldi Lumbricidák a Magyar Nemzeti Múzeumban" (in Hungarian; translated title: Endemic and non-endemic lumbricids of the Hungarian National Museum in Budapest). *Annales Historico-Naturales Musei Nationalis Hungarici*, 36: 12-24.

Qiu, Jiangping & Bouché, Marcel. (1998): "Contribution à la révision des Lumbricoidea (Annelida: Oligochaeta). Une nouvelle sous-espèce du genere *Fitzingeria* Zicsi, 1978". *Documents pedozoologiques & integrologiques* 4: 98–101.

Rabitsch W. & Essl F. (2009). "Endemiten. Kostbarkeiten in Österreichs Pflanzen- und Tierwelt". Klagenfurt und Wien: Naturwiss. V. f. Kärnten u. Umweltbundesamt GmbH, 923 pp.

Ratnasingham, S., Herbert, P. (2007). "BOLD: The Barcode of Life Data System (www.barcodinglife.org)". *Molecular Ecology Notes* 2007, 1-10.

Rawson, S. D., Maksimcuka, J., Withers, P. J., & Cartmell, S. H. (2020). "X-ray computed tomography in life sciences". *BMC Biology*, 18(1), 21.

Ronquist, F.; Teslenko, M.; van der Mark, P.; Ayres, D.; Darling, A.; Höhna, S.; Larget, B.; Liu, L.; Suchard, M.; Huelsenbeck, J. (2012). "MRBAYES 3.2: Efficient Bayesian phylogenetic inference and model selection across a large model space". *Systematic Biology* 61, 539-542.

Rosa, D. (1893). "Allolobophora platyura depressa". *Memorie della Accademia delle scienze di Torino* 43, p. 439.

Rote-Liste-Zentrum (2023). Species entry: *Octolasion tyrtaeum* (Savigny 1826). Available from: https://www.rote-liste-zentrum.de/de/Detailseite.html?species_uuid=0a6d7e14-070c-40ca-b619-60080f0e96a1 (last visited May 21st 2023).

Rutgers, M., Orgiazzi, A., Gardi, C., Römbke, J.; Jänsch, S.; Keith, A. M.; Neilson, R.,; Boag, B.; Schmidt, O., Murchie, A.; Blackshaw, R.; Pérès, G.; Cluzeau, D.; Guernion, M.; Briones, M.; Rodeiro, J.; Piñeiro, R.; Cosín, D.; Sousa, J.; Zwart, D. (2016). "Mapping earthworm communities in Europe". *Applied Soil Ecology* 97, 98–111.

Schindelin, J.; Arganda-Carreras, I.; Frise, E.; Kaynig, V.; Longair, M.; Pietzsch, T.; … Cardona, A. (2012). "Fiji: an open-source platform for biological-image analysis". *Nature Methods* 9 (7), 676–682.

Szederjesi, T.; Pop, V.; Pavlíček, T.; Márton, O.; Krízsik, V.; Csuzdi, C. (2018). "Integrated taxonomy reveals multiple species in the Dendrobaena byblica (Rosa, 1893) complex (Oligochaeta: Lumbricidae)". *Zoological Journal of the Linnean Society* 182 (3), 500–516.

Tamura, K.; Stecher, G.; Kumar, S. (2021). „MEGA11: Molecular Evolutionary Genetics Analysis, version 11". *Molecular Biology and Evolution* 38 (7), 3022–3027.

Thermo Fisher Scientificic. (2020). *Amira 2020.2*. Waltham, Massachusetts, USA.

Westheide, W.; Purschke, G. (2013). „Annelida, Ringelwürmer". In: Westheide, W.& Riege, G. (Hg.). *Spezielle Zoologie* (3. Aufl.). Berlin Heidelberg: Springer Spektrum, 357-415.

Westheide, W. & Rieger, G. (2013). *Spezielle Zoologie* (3. Aufl.). Berlin Heidelberg: Springer Spektrum.

Zicsi, A. (1994). „Die Regenwürmer Österreichs (Oligochaeta: Lumbricidae) mit Bestimmungstabellen der Arten“. *Verhandlungen Der Zoologisch-Botanischen Gesellschaft in Wien* (131), 37–74.
Zicsi, A. (1978). “Fitzigieria”. *Acta Zoologica Hungaricae* (24).
Zicsi A. (1978). ”Revision der Art Dendrobaena platyura (Fitzinger, 1833) (Oligochaeta: Lumbricidae)”. *Acta Zoologica Academiae Scientiarum Hungaricae* 24: 439–449.
Zicsi, A. (1991). ”Über die Regenwürmer Ungarns (Oligochaeta: Lumbricidae) mit Bestimmungstabellen der Arten”. *Opuscula Zoologica Budapest* 24: 167–191.
Zott, D. (2014). *Entwicklung eines molekularen Bestimmungsschlüssels für Regenwürmer des Great Smoky Mountain National Park.* Diplomarbeit an der Universität Innsbruck am Institut für Ökologie.

I have tried my best to find and cite all authors of the images that were adapted used in this project and to obtain their consent to use their images in this project. Should there still emerge any copyright infringements, I kindly ask to contact and notify me.

Ich habe mich bemüht, sämtliche Inhaber*innen der Bildrechte ausfindig zu machen und ihre Zustimmung zur Verwendung der Bilder in dieser Arbeit eingeholt. Sollte dennoch eine Urheberrechtsverletzung bekannt werden, ersuche ich um Meldung bei mir.

Appendix

Abstract in English

Earthworms are of great ecological importance and are known as great soil improvers. In earthworm populations, juvenile earthworms, that do not exhibit fully matured reproductive organs, form the vast majority. In morphological identification keys, juvenile earthworms, however, have been claimed to be unidentifiable as they seemed to lack reproductive morphological features in macroscopic analysis and dissections. This project aims to use MicroCT scanning to search for diagnostic morphological features in 3 adult and 3 juvenile Austrian earthworm specimens and attempt identification. The method of MicroCT scanning will thereby be tested and verified with DNA-barcoding of the CO1 sequences of each specimen. Data have shown that most of the diagnostic morphological features are visible in both adult and juvenile earthworm specimens and that the identification of two juvenile *Fitzingeria platyura platyura* specimens and one juvenile *Lumbricus terrestris* specimen was possible with MicroCT scanning and verified with DNA-barcoding.

Keywords: juvenile lumbricid earthworms, MicroCT scanning, earthworm taxonomy

Abstract in German

Regenwürmer sind bekannt für ihre ökologische Bedeutung als Bodenverbesserer. Regenwurmpopulationen bestehen zum größten Teil aus juvenilen Individuen, die noch keine voll ausgereiften reproduktiven Organe aufweisen. In morphologischer Bestimmungsliteratur wurden sie daher bisher als unbestimmbar deklariert, da ihnen die wesentlichen reproduktiven Merkmale zu fehlen schienen in markoskopischen Analysen und Sektionen. Dieses Projekt wird versuchen, MircoCT scanning für die Suche nach diagnostischen morphologischen Merkmalen in 3 adulten und 3 juvenilen österreichischen Regenwürmern anzuwenden und diese zu bestimmen. Die Methode des MicroCT scanning wird hierbei getestet und verifiziert mittels Bestimmung anhand von DNA-barcoding der CO1-Sequenzen der Regenwürmer. Die Ergebnisse zeigen, dass die meisten diagnostisch-relevanten morphologischen Merkmale in sowohl den adulten als auch den juvenilen Regenwürmern sichtbar sind und dass die Bestimmung zweier juveniler *Fitzingeria platyura platyura* und eines *Lumbricus terrestris* mittels MicroCT scanning möglich und mittels DNA-barcoding verifizierbar war.

Keywords: juvenile Lumbricidae Regenwürmer, MicroCT scanning, Regenwurmtaxonomie

Data availability

 Specimen data can be accessed via the University of Vienna Zoological Collection under the sample IDs UVZC_EV696; UVZC_EV692; UVZC_EV693; UVZC_EV694; UVZC_EV695; UVZC_EV691. The MicroCT scanning images are available via Zenodo (https://zenodo.org/) under 10.5281/zenodo.8033944 under CC-BY license. 3D reconstructions are available upon request.

Acknowledgements

I would like to thank the following people and institutions for their support during this project. First and foremost, Gerhard Steiner for supervising and Brian Metscher for supporting the MicroCT scanning process. Big thanks also to Christan Baranyi for primer design and to Simon Engelberger for archiving the specimens. I want to thank Thomas Schwaha, Julian Biebermair, and Sophie Greistorfer for their support with imaging software. My gratefulness also goes out to Julia Bauder and Nadja Hattinger for supporting me with the lab work, and to the team of the Department of Evolutionary Biology for supporting me with my many questions. I want to thank my parents and grandparents for their love and support, my sister for her love and excitement and helping hand during fieldwork, and my partner for his patience, love, and support. I thank my colleagues at Mittelschule Jochbergengasse, especially Barbara Bauer and Dilara Özdemir, for their support and understanding during my most intense writing phases. And finally, I want to thank my friends for their patience and support during this year and for motivating me to finish.